

1. Introduction

1.1 Stress Concentration

In a loaded structural member, near changes in the section, distributions of stress occur in which the peak stress reaches much larger magnitudes than does the average stress over the section. This increase in peak stress near holes, grooves, notches, sharp corners, cracks, and other changes in section is called stress concentration.

In any case where an abrupt change is present in geometry of an object subjected to loading, the Stress distribution does not remain uniform concentration arises. These openings and cutouts result in strength degradation of the structure which may lead to unexpected and early failure of the component. Therefore it is seemed to be very important to study the stress concentration factor (SCF) in cases where an abrupt change is present in the component. Stress concentration factor serves as a multiplication factor and used to find the value of maximum stress produced in the geometry. It is defined as the ratio of the calculated peak stress to the nominal stress that would exist in the member if the distribution of stress remained uniform. Thus in case of transverse loading, SCF is given by:

$$SCF = \frac{\sigma_{\text{maximum}}}{\sigma_{\text{nominal}}} \quad (i)$$

In many engineering fields such as in aerospace engineering, marine engineering, automobile engineering plate under in-plane loading condition have widespread use but many times the plate is also provided with a central circular hole for the provision of bolts, rivets etc. This hole acts as discontinuity due to which a significant increase in the maximum stress level is observed and the stress concentration factor comes into play. As a result the components may fail due to fatigue crack propagation or large deformations at those stress concentration points. Therefore analysis of stress concentration factor developed at those highly stressed regions becomes very necessary. As high SCF developed in a body lead to unexpected failure of the component it is also important to reduce SCF developed in the body. Studies are available on analysis of stresses in plates with circular holes but limited methods are reported in the direction of reduction of stress concentration factor.

1.2 Finite Element Method

The Finite Element Analysis is a computational technique used to obtain approximate solutions of boundary value problems in engineering by discretization of a continuous problem. A boundary value problem or a field problem is a mathematical problem in which one or more dependent variables must satisfy a differential equation everywhere within a known domain of independent variables and satisfy specific conditions on the boundary of the domain.

The Finite Element Method constitutes of three important stages, the pre-processing stage, the solution stage and the post-processing stage. These stages are explained in detail in the following sections:

(a) Pre-Processing: In the pre-processing stage, a computer-aided design model of the real-time problem of any nature, be that structural, thermal, fluid, electromagnetic, etc is created. The model, after being created, is divided into small discrete pieces known as elements. These elements are joined together at nodes and a combination of these nodes and elements forming the model is known as a mesh. The meshed model is then subjected to all the conditions being applied to the real-time problem. The conditions may be several types of fixtures and several types of loadings. These may be single or multiple, depending upon the problem being undertaken to be solved. These conditions are known as the boundary conditions as they are applied at the boundary or the surface of the formed mesh and not at the inter-elemental nodes.

(b) Solution: The model is set to solve in the required mode of solution. The model takes some time to solve. This solution time depends on the number of elements created after meshing. More the number of elements created, more is the time taken for the solution. After the solution, the post-processing is done to extract the required results.

(c) Post-Processing: The post processing is done in order to extract the required results from the generated results. The first stage of post-processing is the Mesh-Dependence Test and the second stage is the generation of results in the converged mesh size. The solution phase generates all types of displacements, stresses, strains, strain energies, etc. In the post processing phase, the required results are extracted, noted and studied, so that the results can be inferred and concluded.

1.3 Photoelasticity

All crystal other than those of cubic crystal possesses one property called double refraction or birefringence. Birefringence is an event when a ray of light, which is incident on certain crystals, is split into two components. The two components are then transmitted through the crystal in different directions. If the two rays have passed through the crystal are observed through an analyser, it is found that they are plane polarized in mutually perpendicular planes.

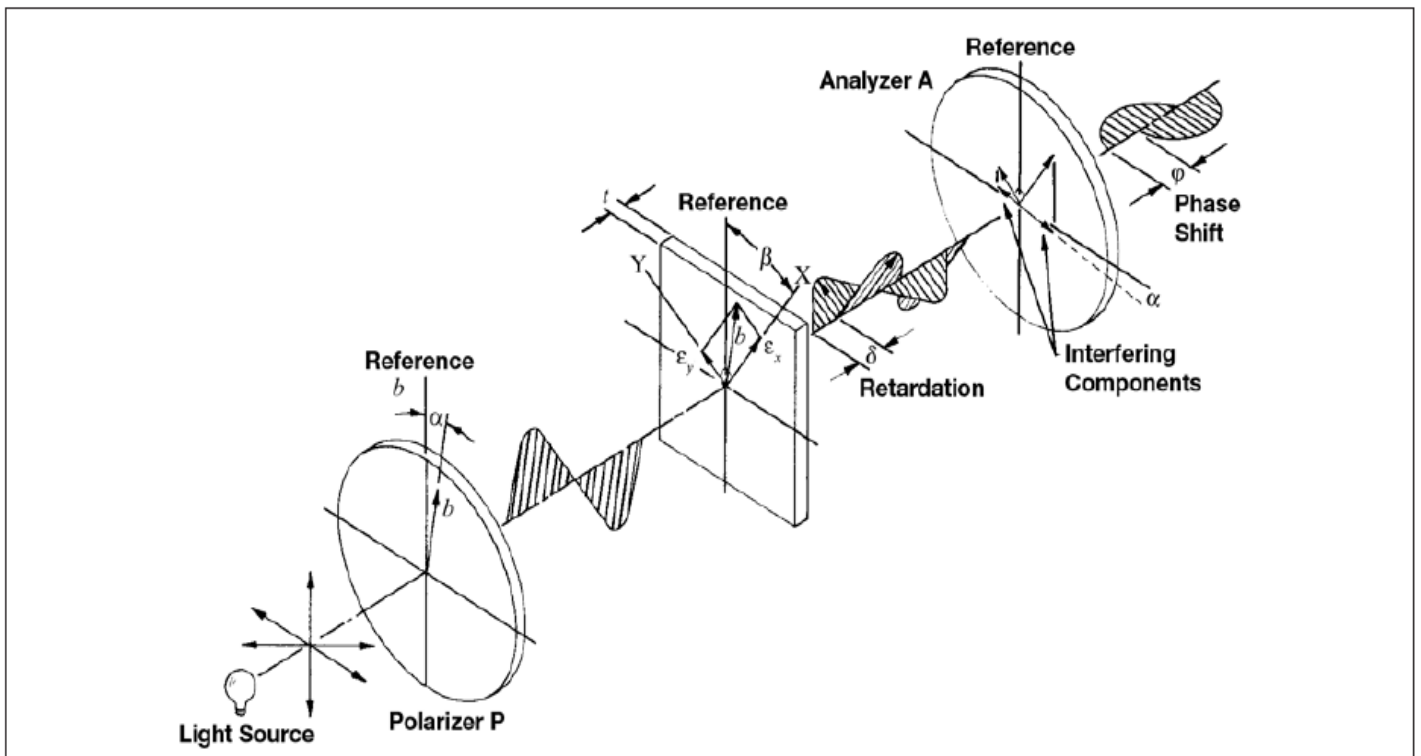


Fig.1 Polarisation of light

It is one of the most powerful experimental methods for two dimensional as well as three dimensional stress analysis. The name photoelasticity reflects the nature of this experimental method, photo implies the use of light rays and optical techniques, while elasticity depicts the study of stresses and deformations in elastic bodies.

The photoelastic method is based upon a unique property of some transparent materials, in particular, certain plastics. Consider a model of some structural part made from a photoelastic material. When the model is stressed and a ray of light enters along one of the directions of principal stress, a remarkable thing happens. The light is divided into two component waves, each with its plane of vibration (plane of polarization) parallel to one of the remaining two principal planes (planes on which shear stress is zero). Furthermore, the light travels along these two paths with different velocities, which depend upon the magnitudes of the remaining two principal stresses in the material.

The incident light is resolved into components having planes of vibration parallel to the directions of the principal stresses σ_1 and σ_2 . Since these waves traverse the body with different velocities, the waves emerge with a new phase relationship, or relative retardation.

If monochromatic and polarized light is incident on the loaded photoelastic model then optical interference of the two light rays will occur. This can be achieved by using a polariscope. Therefore when the loaded model is seen through the polariscope then due to optical interference the light intensity will be maximum at a point and minimum at the other point. The light intensity at different location of in the loaded object is given by the equation of two-beam interference.

$$I = a^2 \cos^2 \pi N \quad (ii)$$

(where N is fringe order or relative retardation)

If the relative retardation N is 0, 1, 2, 3... cycles, the waves reinforce each other, and the combined effect is a large light intensity. If the phase difference N is $1/2$, $3/2$, $5/2$, $7/2$,... cycles, the amplitude of the two interfering waves is everywhere equal and opposite and the light intensity diminishes to zero

(extinction) due to destructive interference. Unlike the analytical methods of stress determination, photoelasticity gives a fairly accurate picture of stress distribution even around abrupt discontinuities in a material. The method serves as an important tool for determining the critical stress points in a material and is often used for determining the stress concentration factors in irregular geometries.

The fundamental of stress optic law was first introduced by sir Devid Brewster in the early 1800's but the theory which relates the change of refractive indices to the applied mechanical stresses were established by Maxwell and Newman. In 1853, Maxwell related the birefringence to stress through the stress-optical law which is expressed in equation:

$$\sigma_1 - \sigma_2 = \frac{\lambda}{2\pi t C} \delta \quad (iii)$$

(where σ_1, σ_2 are the two principal stresses)

C is the stress-optic coefficient,

t is the thickness of the sample,

λ is the wavelength of the light source and

δ is the phase difference between the two refracted rays and is called phase retardation.

On further simplification:

$$\sigma_1 - \sigma_2 = \frac{f_\sigma N}{t} \quad (iv)$$

These formula is known as stress-optic law

where,

$N = \frac{\delta}{2\pi}$ is fringe order,

$f_{\sigma} = \frac{\lambda}{c}$ is the Material fringe value and

t is the thickness of the specimen.

In case of uniaxial stress system, at the edge of hole

$$\sigma_2 = 0$$

$$\sigma_1 = \frac{f_{\sigma} N}{t} \quad (v)$$

$$\sigma_{nominal} = P/(A - D)t \quad (vi)$$

Where

P = Applied load on specimen

A = Plate Width

D = Diameter of circular hole

t = thickness

$$SCF = \sigma_{actual}/\sigma_{nominal} \quad (vii)$$

$$SCF = \frac{f_{\sigma} N(A-D)}{P} \quad (ix)$$

2. Literature Review

A. J. Durelli and K. Rajaiah[1]

This paper presents optimized hole shapes in plates of finite width subjected to uniaxial load for a large range of hole to plate widths (D/W) ratios. The stress concentration factor for the optimized holes decreased by as much as 44% when compared to circular holes. Simultaneously, the area covered by the optimized hole increased by as much as 26% compared to the circular hole. The geometries of the optimized holes for the D/W ratios is considered. It is also suggested that the developed geometries may be applicable in the cases of rectangular holes and also for the tip of a crack.

K. Rajaiah and N. K. Naik[2]

An isotropic plate having central circular hole is taken and tensile uniaxial load is applied. Research technique used is photo elastic method and it was found that for a central-hole diameter-to-plate width ratio of 0.222 there is upto 30% reduction by original hole shape optimization & 23 % reduction by auxiliary hole shape optimization.

Troyani , n. Et al[3]

The work has been carried out to find out theoretical stress concentration factor in a rectangular plate with central circular hole subjected to uniform tension using the finite element method. For same (a/w) ratio theoretical has been determined for the plate with short length and long length by the formula

$$K_t = \text{maximum stress} / \text{nominal stress}$$

It is concluded in the paper that the length of the loaded member may have a large influence on the distribution of stresses near the vicinity of geometric holes, notches, etc. and as a result on the maximum stress there consequently this parameter must be included in either stress analysis or design procedures for short plates.

Shubhrata Nagpal, Nitin Jain and Shubhashis Sanyal- Stress concentration and its mitigation techniques in flat plate with singularities [4]

The size of elliptical hole i.e. b/a ratio affects is considered. As the size of elliptical hole with respect to width of plate i.e. a/A increases the stresses also increase. As b/a ratio increases the stresses decreases from which it is concluded that as the sharpness of ellipse reduces the stresses decreases. The stresses reported are more in case of ellipse as compared to circle for same loading conditions. The area reduction method can be applied for mitigation of SCF around the ellipse.

The introduction of auxiliary holes reduces the SCF on elliptical hole as it causes the smooth stiffness changes along the direction of acting force is beneficial to the decrease of the stress concentration. The distance and size of circular holes effects the mitigation of SCF around the elliptical hole. The increase of number of auxiliary circular holes around the ellipse along the direction of applied force is beneficial for the mitigation of stress concentration. The maximum reduction in SCF has been reported when the auxiliary holes are placed near to the elliptical hole and are of equal to minor axis of the ellipse.

S. A. Meguid[5]

Isotropic plate with two coaxial holes were used, which was uniaxially loaded. Reduction of the stress concentration factor is analyzed by finite element method. Three systems for defence holes were described. Reduction in maximum SCF ranging from 7.5 to 11 % has been achieved.

Kambale and Gulhane[6]

They performed some work on Relief holes for the mitigation of stress concentration factor of a thin rectangular plate under in-plane loading. The reduction in SCF is achieved by introducing one set of auxiliary hole on both side of main hole. The finite element formulation is carried out by using the software Hypermesh.

N.K. Jain et al.[7]

They demonstrated the optimize design of a square simply supported isotropic plate with central circular hole for reduction of stress concentration subjected to transverse static loading using finite element method. In this work the stress concentration is reduced by removal of material from the plate in the form of circular and oval cavities.

Heywood [8]

He explained that introduction of small holes in either side of the original hole helps in smoothening the tensile principal stress trajectories past the original hole which in turn reduces the concentration of stress.

Banerjee et al.[9]

They investigated the effect of fibre orientation on the SCF in fibrous composite plates with central circular hole under transverse static loading condition. The effects of thickness-to-width (T/A) and diameter-to-width (D/A) ratios upon SCF at different fibre orientation are studied. The finite element formulation and its analysis were carried out using ANSYS package.

A. I. Zirka[10]

He took orthotropic plate having circular hole and used photoelastic method For analysis. He applied static and dynamic loads and found Experimental & theoretical values, of dynamic SCF & static SCF are similar. Dynamic SCF can be approximately found by using static SCF & dynamic elastic characteristic of the material.

3. Research Gap

- For reduction in stress concentration factor in rectangular plate having circular hole subjected to in-plane loading, till now more focus is given to change in shape of main hole or position of auxiliary circular holes around the main hole.
- In the Ph.D thesis, S. Nagpal reported 18-22% reduction in SCF by introducing a series of auxiliary holes as shown in fig.(a).
- A reduction of 28% in SCF is also achieved in the work of S. Nagpal but with changing the basic hole shape, as shown in fig.(b).

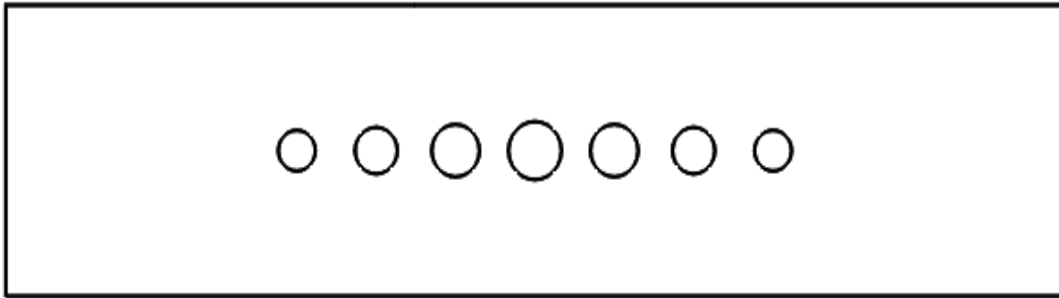


Fig.(a)

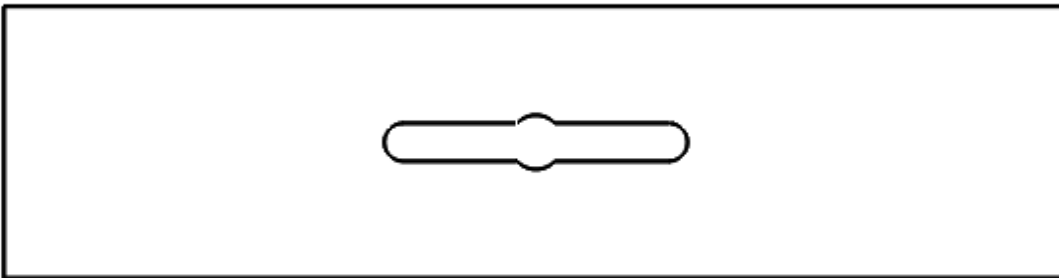


Fig.(b)

- In present work, we have considered a trapezoidal shaped auxiliary hole in the direction of application of load. By using the trapezoidal shaped auxiliary hole, significant reduction in stress concentration factor is observed. The result obtained from finite element method (ANSYS) is validated by performing photo elasticity experimentation.

Research objectives:

- a)* To reduce the Stress Concentration Factor (SCF) in plates with central circular hole subjected to in-plane loading through trapezoidal holes.
- b)* To compare the results obtained from ANSYS with those inferred from the photoelasticity experiment.
- c)* To plot the graph for stress concentration factor by changing the various parameters of trapezoidal hole.
- d)* To find the optimum design by changing the parameters of trapezoidal hole.

4. Methodology

The SCF is reduced by introducing two auxiliary holes are around the main hole. (a) is the main plate which contains a circular hole at the centre and (b) is the optimized design of the plate in which trapezoidal holes are introduced around the main hole to reduce SCF. (c) illustrates the model with their loading and boundary conditions.

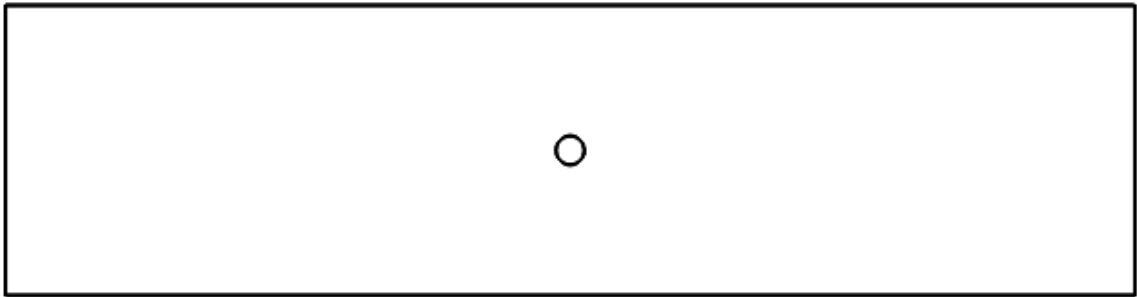


Fig.2 Model (a)

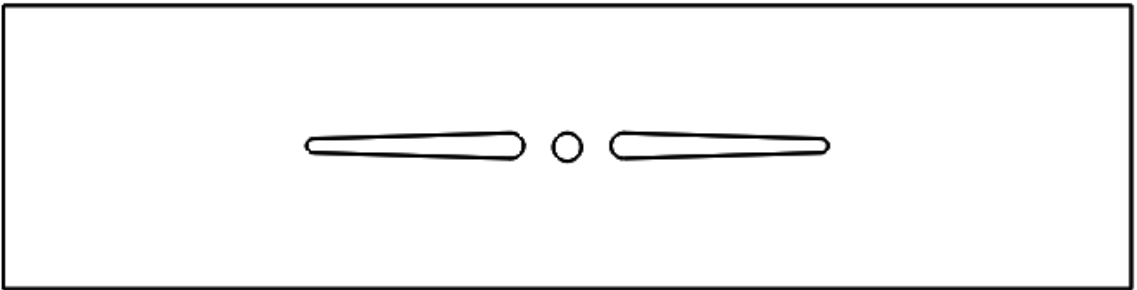


Fig.3 Model (b)

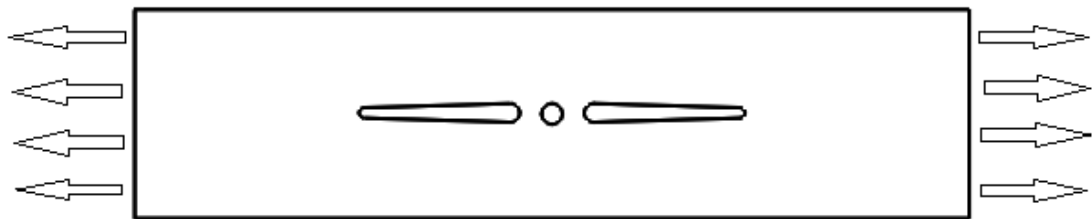


Fig.4 Model (c)

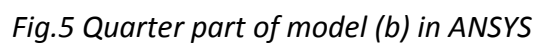
4.1 Methodology of Finite Element Analysis:

- *Process steps:*
 1. Start Mechanical APDL
 2. Preference (structural and h-method)
 3. Pre-processor
 - a) Element type: solid-8 node 183
 - b) Material Properties: Material Model: isotropic
 - c) Modelling: Create surface
 - d) Meshing: free mesh and give element size
 - e) Load: (i) Displacement on boundary and symmetric boundary
(ii) Pressure on line
 4. Solution
 - a) Analysis Type: Structural
 - b) Analysis Option
 - c) Solve
 5. Post Processing: Result and Summary.

The present solution is based on two approaches, finite element method and 3D photoelastic method. In the present research work two dimensional analysis is done. The two dimensional analysis of the models are done using 8 noded solid 183 element type. The element is defined by 8 nodes having two degrees of freedom per node, translations in the nodal x and y directions.

Due to the symmetric nature of different plates investigated, it was only necessary to analyze the quarter part of the plate for finite element analysis. The discretized model of quarter plate is presented in figure. As the whole analysis is performed on quarter plate so symmetric boundary conditions are applied on corresponding edges along which the plate is symmetric. The effect of auxiliary holes on reduction of SCF is to be investigated here. In finite element analysis

The in-plane loading and the boundary conditions applied for model i.e. for solid plate is shown in figure. As the FEM analysis is done on the quarter part of the models so symmetric boundary conditions have also been applied on corresponding edges of the quarter models as shown in the figure below.


$$\% \text{ Reduction in SCF} = \frac{(\text{SCF})_{\text{model(a)}} - (\text{SCF})_{\text{model(b)}}}{(\text{SCF})_{\text{model(a)}}} \quad (x)$$

4.2 Methodology of Three dimensional photoelastic analysis:

The three dimensional photoelasticity method is used for the experimental stress analysis of the models. This method has been considered to be one of the most powerful experimental method for stress analysis. The method involves casting of plates, cutting of holes in the plate and photoelastic analysis.

(a) Plate Casting:

For casting process a mould and casting material is required. The mould is prepared by placing a C bracket in between two flat plate. The inside dimension of the C bracket is same as that of the plate required to prepare the models. The material is poured from the open side of the C bracket. This is fixed between the other two plates but the before that they are covered by smooth plastic sheet to have better finish in the product.

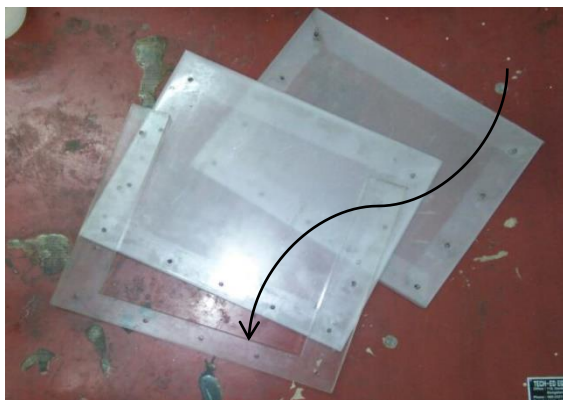


Fig.6 Mould plates



Fig.7 Assembly of mould plates

Photoelastic material is used as casting material of the plates which provides optical response upon application of stress. This material is prepared by mixing two constituent solutions together in right proportions. Here Araldite CY-230 and Aradur HY-951 are mixed in 7:1 ratio to prepare the casting material and

then it is poured into the mould. The mixture solution is stirred slowly so that bubble do not form. Then it is slowly poured into the mould and kept undisturbed for atleast 16 hours to solidify.



Fig.8 Materials required

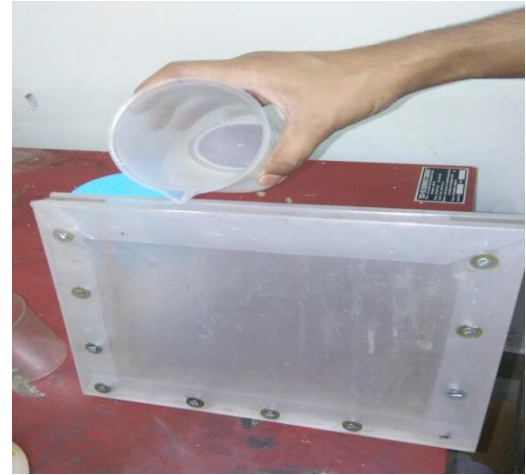


Fig.9 Pouring of solution

Two square plates for these models are casted by the above procedure. From the two plates, four rectangular plate models and two disc models are cut. The two circular discs were prepared during casting of plates to find the material fringe value (f_{σ}).

(b) Model preparation:

The holes and the auxiliary holes are cut out of the plates to prepare model (a) and model (b).

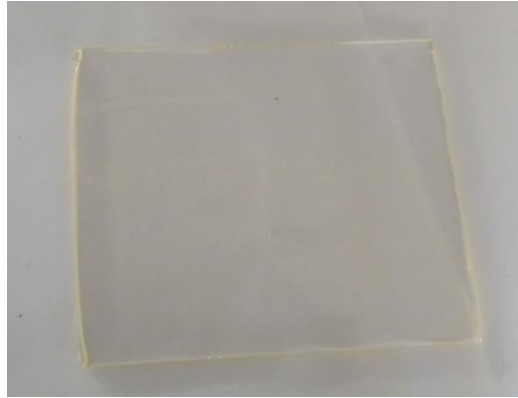


Fig.10 Solid plate



Fig. 11 Model (a) with side holes for holding

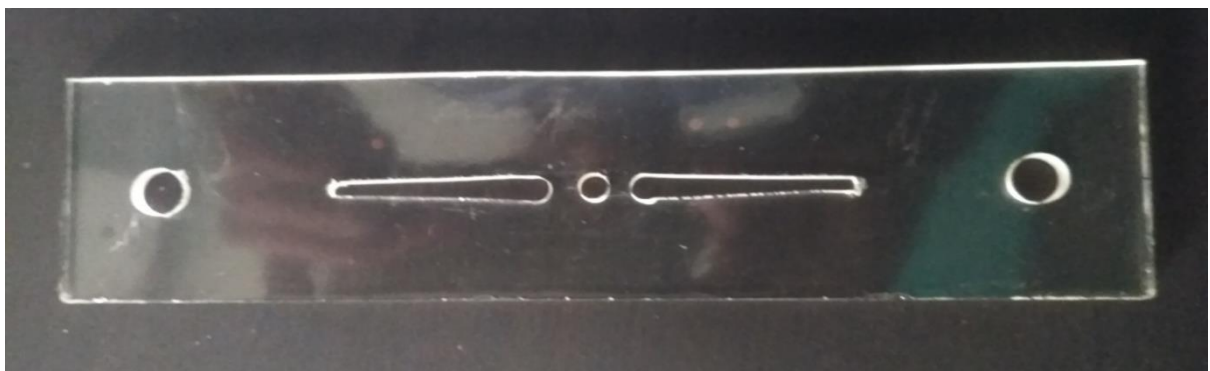


Fig. 12 Model (b) with side holes for holding



Fig. 13 Photoelastic experimentation apparatus

Determination of Material fringe value (f_σ):

The material fringe value (f_σ) is defined as the number of fringes produced per unit load and it is determined by applying diametral load on a calibration circular disc.

$$f_\sigma = \frac{8P}{\pi DN} \quad (xi)$$

where P is single diametral compressive load (in kgf)

D = diameter of the circular disc (in cm)

N = fringe order at the point of interest along the horizontal diameter.

By lever rule:

$$W = \frac{PL_1}{L} \quad (xii)$$

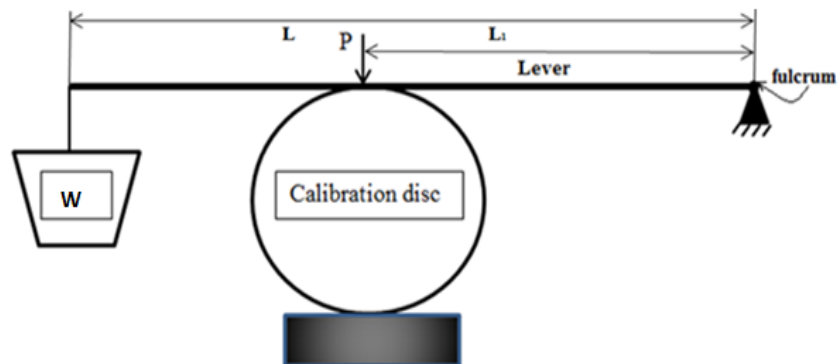


Fig. 14 Calibration disc under diametrical compression


TABLE 1 – ISOCHROMATIC FRINGE CHARACTERISTICS				
Color		Approximate Relative Retardation		Fringe Order
		nm	in x 10 ⁻⁶	<i>N</i>
	Black	0	0.0	0.0
	Pale Yellow	345	14.0	0.60
	Dull Red	520	20.0	0.90
	Red/Blue Transition	575	22.7	1.00
	Blue-Green	700	28.0	1.22
	Yellow	800	32.0	1.39
	Rose Red	1050	42.0	1.82
	Red/Green Transition	1150	45.4	2.00
	Green	1350	53.0	2.35
	Yellow	1440	57.0	2.50
	Red	1520	60.0	2.65
	Red/Green Transition	1730	68.0	3.00
	Green	1800	71.0	3.10

Fig. 15 Determination of fringe order by white light

Experimental procedure:

- Determine material fringe value by using disc.
- Apply load on specimen and note the load for different fringe orders for monochromatic light.
- Perform the above step for white light by using the Table no.1 for finding fringe order.
- Calculate stress concentration factor using equation (ix).

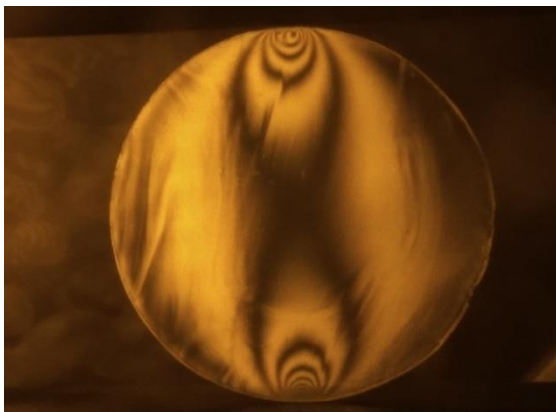
5. Observations and Calculations

5.1 Determination of Fringe Order:

Table.1 Dark fringe- Case I: Diameter of disc 4cm

<i>Fringe order (N)</i>	<i>Apparatus Reading (W in kgf)</i>	<i>Specimen load (P in kgf)</i>	<i>Material fringe value (F_σ in kgf/m)</i>
1	3.68	11.585	741.247
2	9.78	30.789	984.97
3	15.67	49.33	1052.07
4	21.50	67.685	1082.66

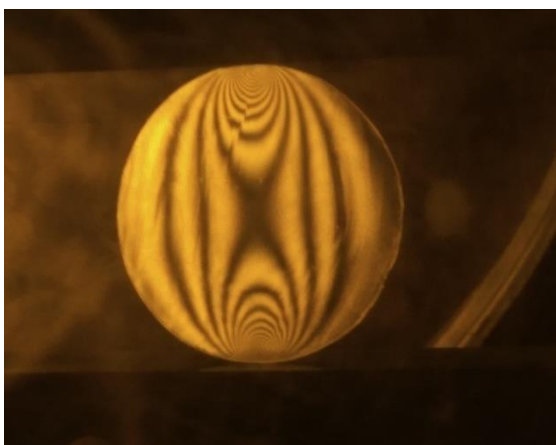
Average material fringe value = 966.23 kgf/m



(b) First order (N=1)



(a) Second order (N=2)



(d) Third order (N=3)



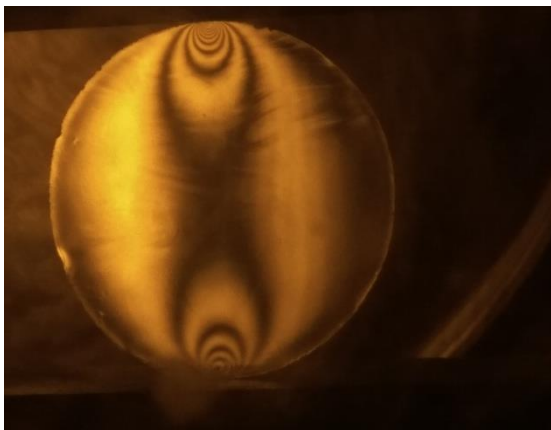
(c) forth order (N=4)

Fig.16 Dark fringe for diameter of disc= 4cm

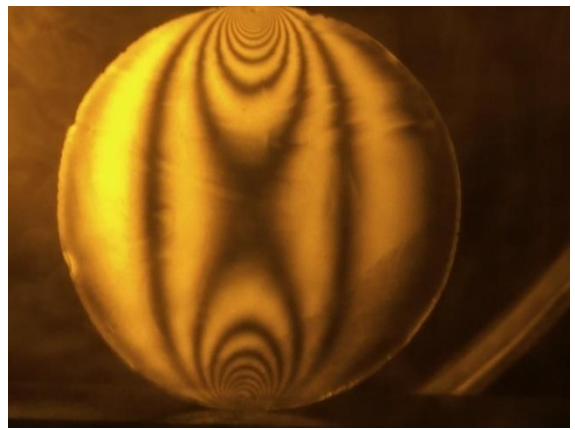
Table.2 Dark fringe- Case II: Diameter of disc 5cm

<i>Fringe order (N)</i>	<i>Apparatus Reading (W in kgf)</i>	<i>Specimen load (P in kgf)</i>	<i>Material fringe value (F_o in kgf/m)</i>
1	5.35	16.84	849.3
2	12.85	40.45	1019.90
3	20.40	64.22	1079.47
4	28.30	89.09	1123.13

Average material fringe value = 1017.96 kgf/m



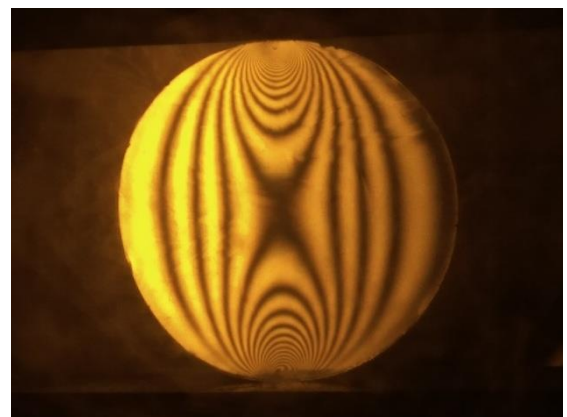
(a) First order (N=1)



(b) Second order (N=2)



(c) Third order (N=3)



(d) forth order (N=4)

Fig.17 Dark fringe for diameter of disc= 5cm

Table.3 Light fringe- Case I: Diameter of disc = 4cm

<i>Fringe order (N)</i>	<i>Apparatus Reading (W in kgf)</i>	<i>Specimen load (P in kgf)</i>	<i>Material fringe value (F_σ in kgf/m)</i>
0.5	2.25	7.083	906.82
1.5	8.5	26.659	1141.96
2.5	14.8	49.59	1193.01
3.5	21.2	66.74	1220.67

Average material fringe value = 1115.61 kgf/m

Table.4 Light fringe- Case II: Diameter of disc = 5cm

<i>Fringe order (N)</i>	<i>Apparatus Reading (W in kgf)</i>	<i>Specimen load (P in kgf)</i>	<i>Material fringe value (F_σ in kgf/m)</i>
0.5	3.3	10.38	1048.05
1.5	11.0	34.63	1164.58
2.5	19.4	61.07	1232.35
3.5	26.7	84.05	1211.48

Average material fringe value = 1139.86 kgf/m

$$\begin{aligned} \text{Overall mean of material fringe value} &= \frac{(966.23 + 1017.96 + 1115.61 + 1139.86)}{4} \\ &= 1065.98 \text{ kfg/m.} \end{aligned}$$

5.2 SCF by Photo elasticity Method:

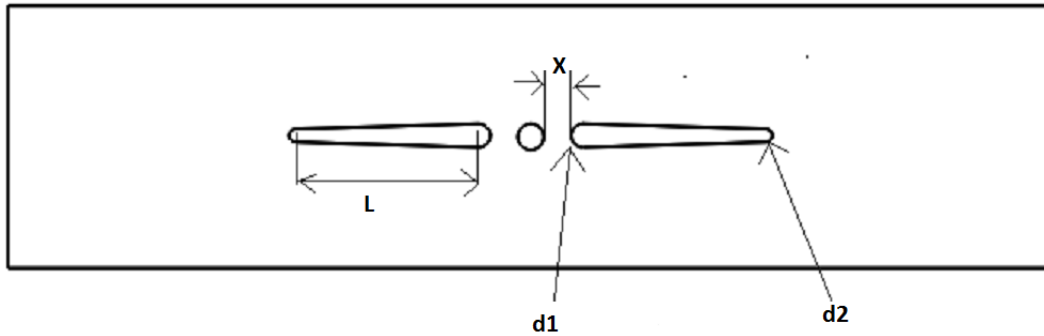


Fig.18 Parameters in plate model

Specimen1: With no auxiliary hole

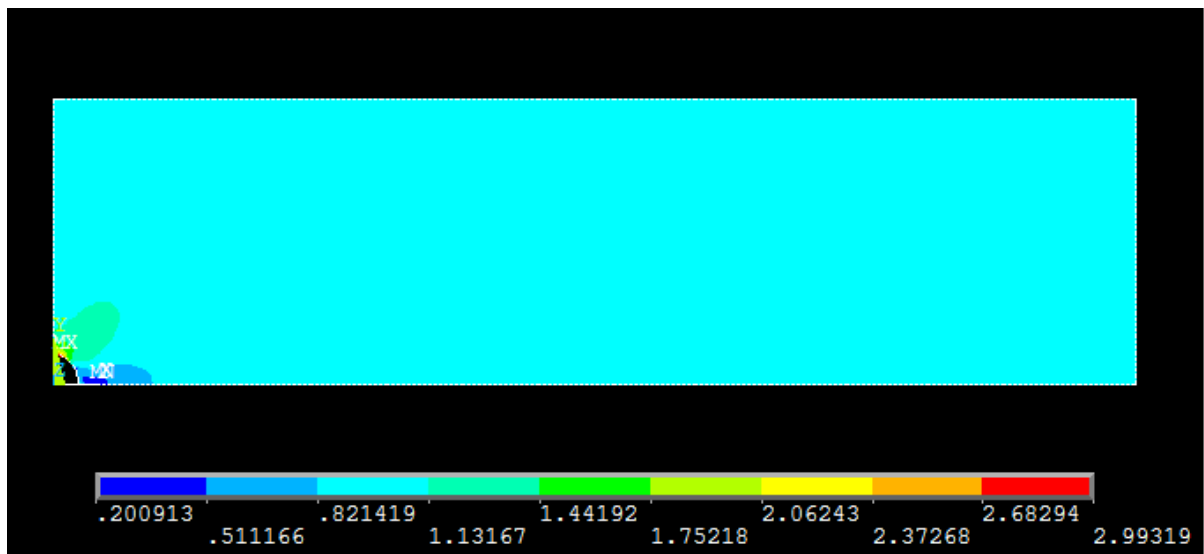


Fig.19 Analysis of specimen1

$$\begin{aligned} \text{SCF} &= 2.99 * 0.9 \\ &= 2.69 \end{aligned}$$

Table.5 SCF from monochromatic light fringe

<i>Fringe order (N)</i>	<i>Apparatus reading (W in kgf)</i>	<i>Specimen Load (P in kgf)</i>	<i>SCF_{experimental}</i>	<i>SCF by ANSYS</i>
1	5.44	17.13	2.8	2.69
2	11.10	34.94	2.75	
3	16.96	54.39	2.66	

Table.6 SCF from white light fringe

<i>Fringe order (N)</i>	<i>Apparatus reading (W in kgf)</i>	<i>Specimen Load (P in kgf)</i>	<i>SCF_{experimental}</i>	<i>SCF by ANSYS</i>
1	5.56	17.50	2.74	2.69
2	11.32	35.58	2.70	
3	17.04	53.64	2.68	

Mean experimental value of SCF= 2.72

Deviation of ANSYS result from Experimental result = 1.1%.

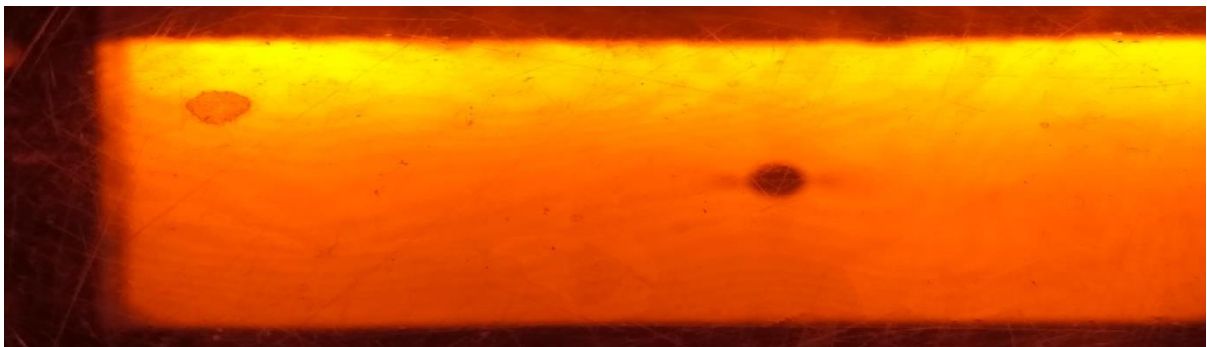


Fig.20 First order fringe (monochromatic)

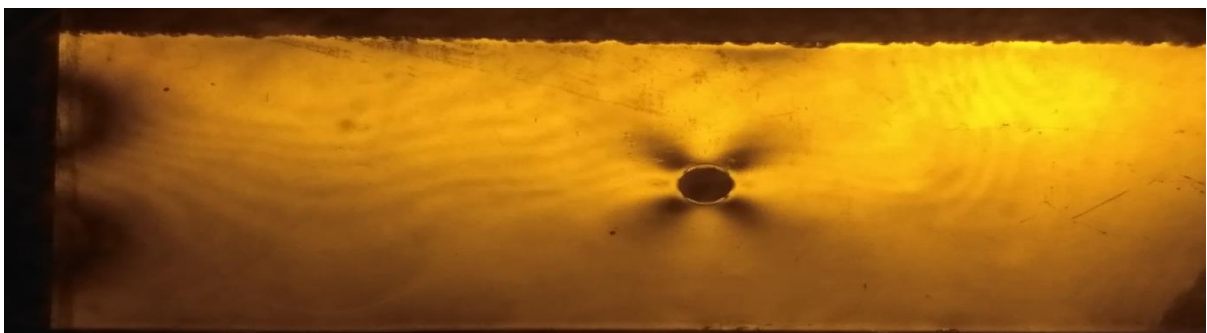


Fig.21 Second order fringe (monochromatic)

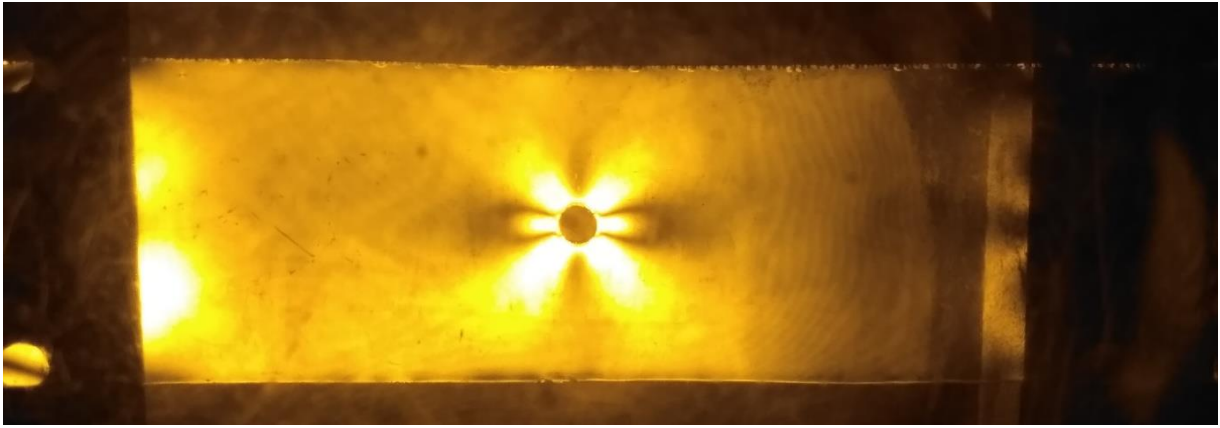


Fig.22 Third order (monochromatic)



Fig.23 First order fringe (white light)

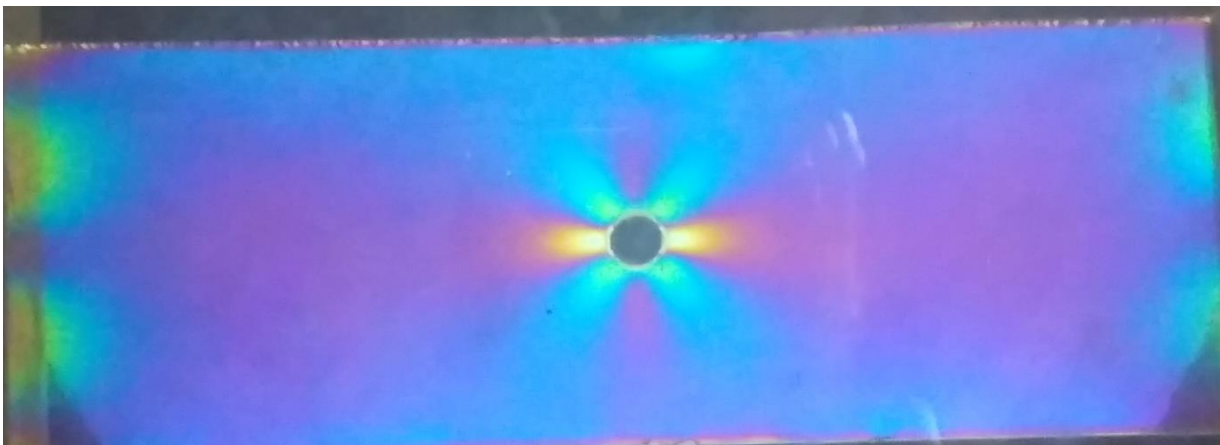


Fig.24 Second order fringe (white light)

Specimen2: X=5mm, L=35mm, d1=5mm, d2=3mm

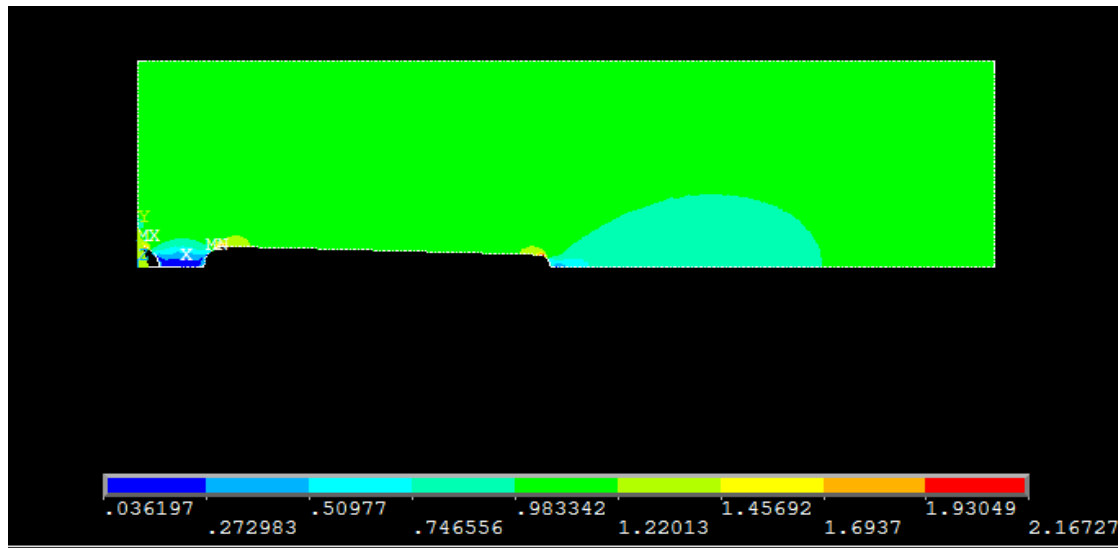


Fig.25 Analysis of specimen2

$$\begin{aligned} SCF &= 2.14 * 0.9 \\ &= 1.95 \end{aligned}$$

Table.7 SCF from monochromatic light fringe

<i>Fringe order (N)</i>	<i>Apparatus reading (W in kgf)</i>	<i>Specimen Load (P in kgf)</i>	<i>SCF_{experimental}</i>	<i>SCF by ANSYS</i>
1	8.01	25.22	1.90	1.95
2	15.67	49.33	1.94	
3	23.77	74.83	1.92	

Table.8 SCF from white light fringe

<i>Fringe order (N)</i>	<i>Apparatus reading (W in kgf)</i>	<i>Specimen Load (P in kgf)</i>	<i>SCF_{experimental}</i>	<i>SCF by ANSYS</i>
1	8.03	25.28	1.90	1.95
2	15.74	49.55	1.94	
3	23.25	73.19	1.96	

Mean experimental value of scf= 1.93

Deviation of Ansys result from Experimental value= 1.0%.

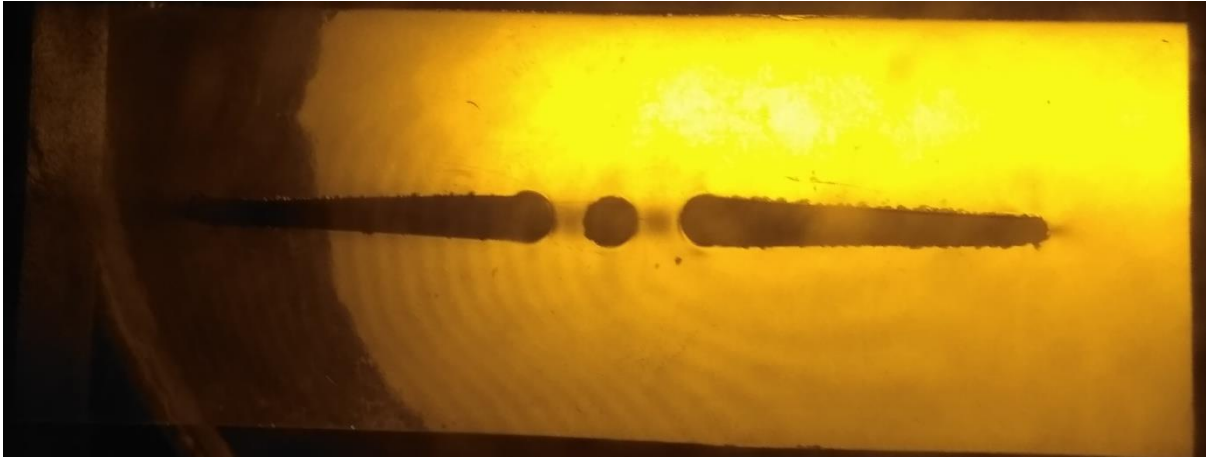


Fig.26 First Order (monochromatic)

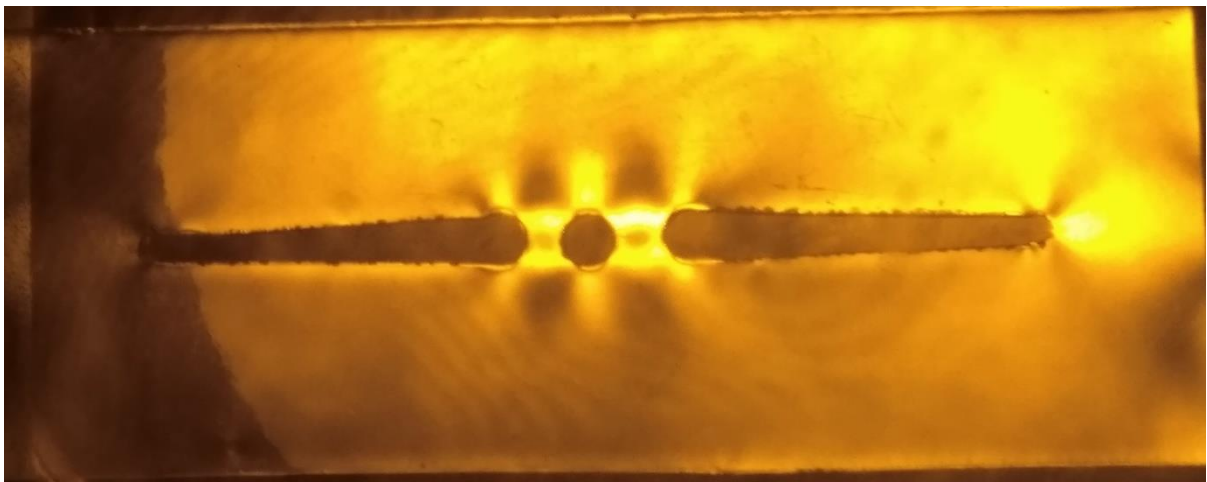


Fig.27 Second Order (monochromatic)

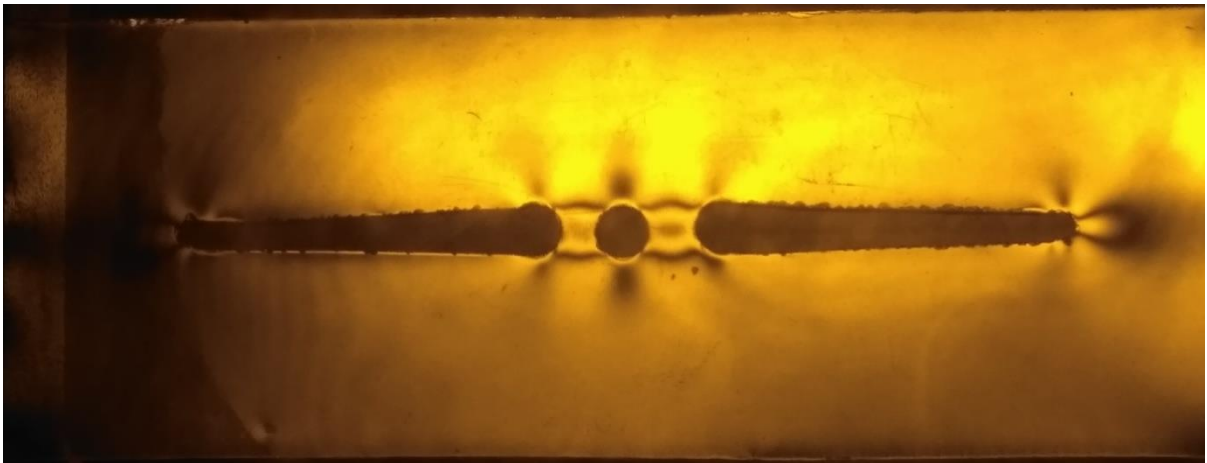


Fig.28 Third Order (monochromatic)

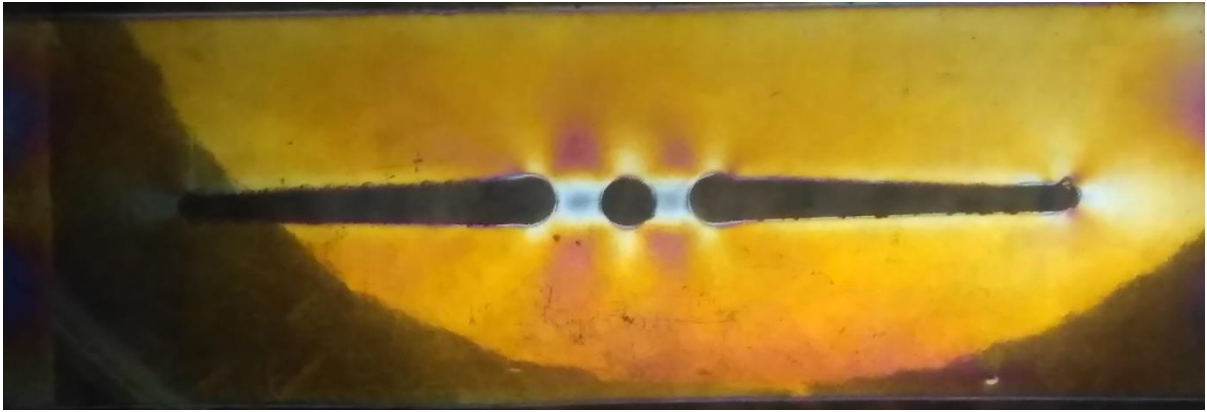


Fig.29 First Order (white light)

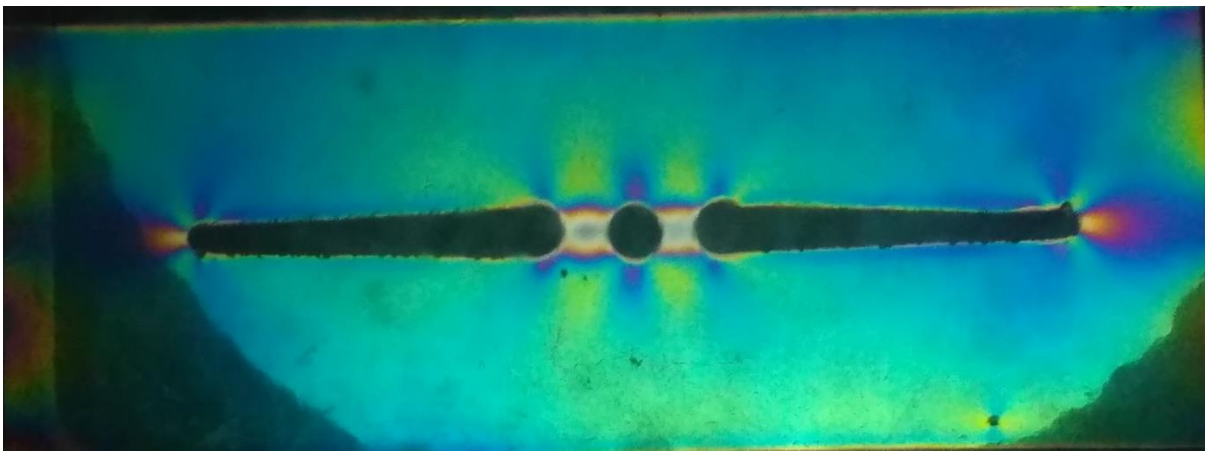


Fig.30 Second Order (white light)

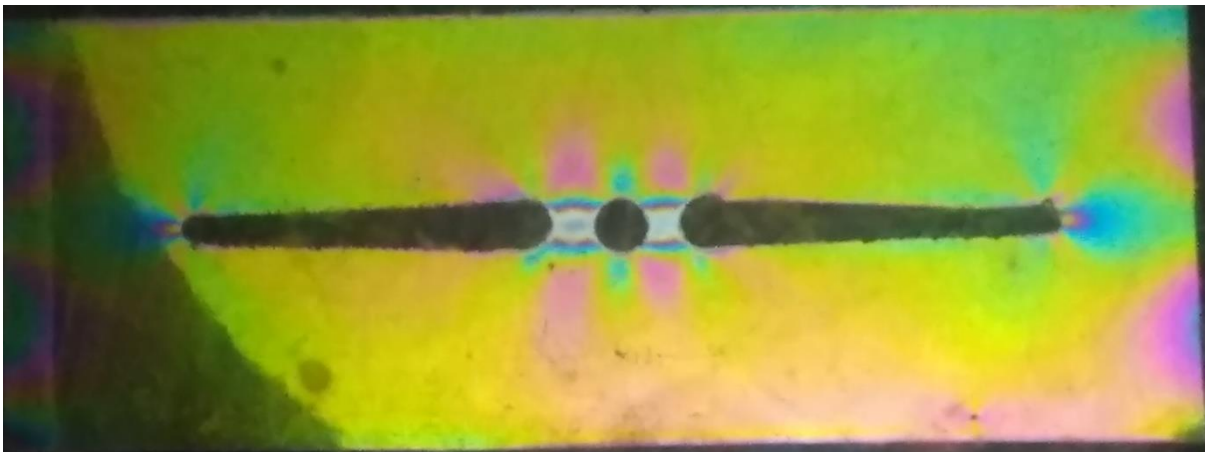


Fig.31 Third Order (white light)

Specimen3: X=5mm, L= 20mm, d1=5mm, d2= 3mm

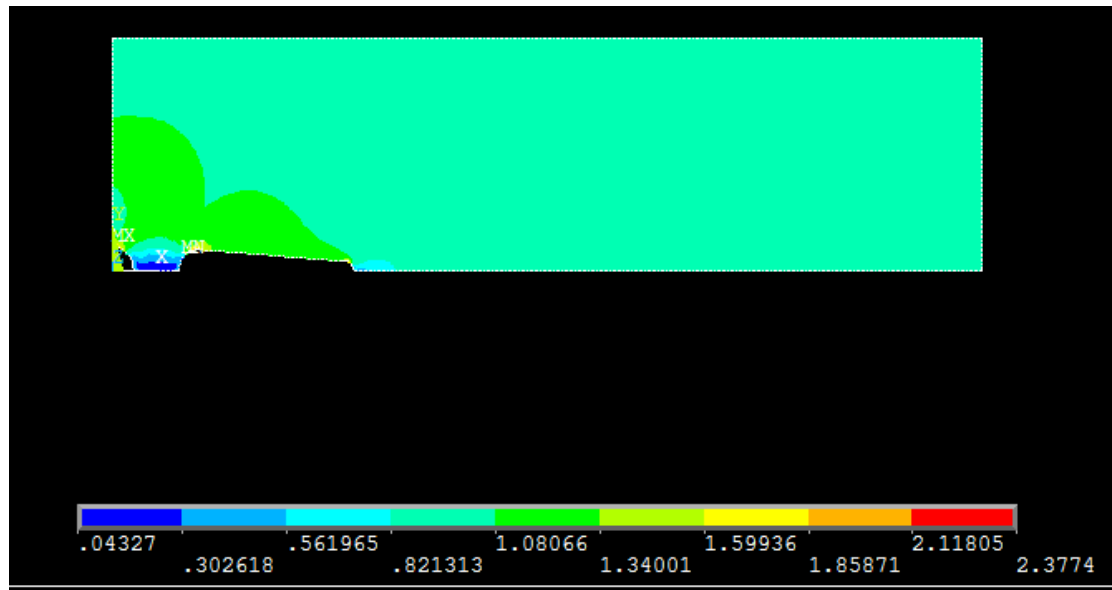


Fig.32 Analysis of specimen3

Table.9 SCF from monochromatic light fringe

<i>Fringe order (N)</i>	<i>Apparatus reading (W)</i>	<i>Specimen Load (P)</i>	<i>SCF_{experimental}</i>	<i>SCF by ANSYS</i>
1	7.46	23.48	2.04	2.14
2	13.7	43.13	2.22	
3	23.2	73.03	1.97	

Table.10 SCF from white light fringe

<i>Fringe order (N)</i>	<i>Apparatus reading (W)</i>	<i>Specimen Load (P)</i>	<i>SCF_{experimental}</i>	<i>SCF by ANSYS</i>
1	7.16	22.54	2.13	2.14
2	14.00	44.07	2.18	
3	23.14	72.84	1.98	

Mean experimental value of scf= 2.09

Deviation of Ansys result from Experimental value= 2.3%

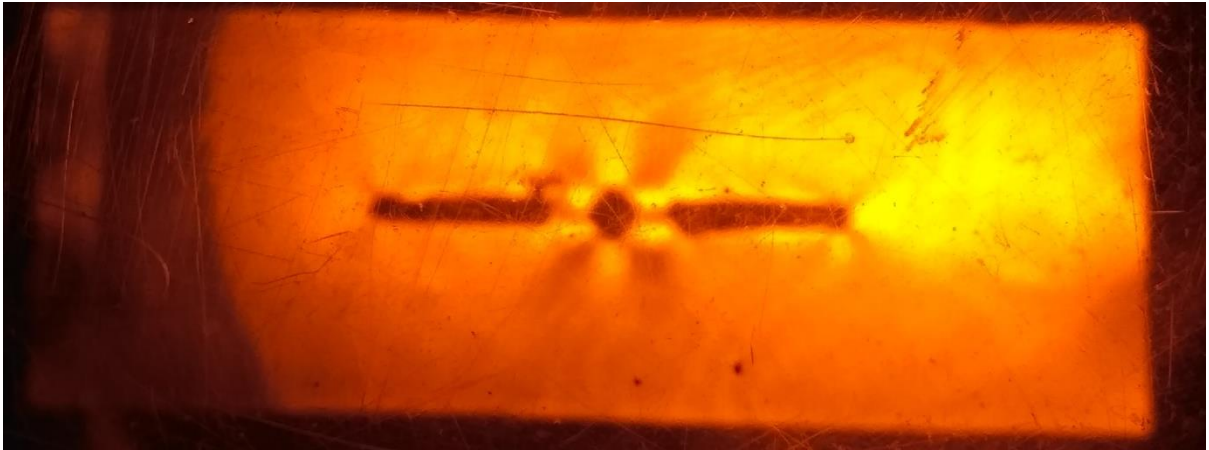


Fig.33 Second Order (monochromatic)

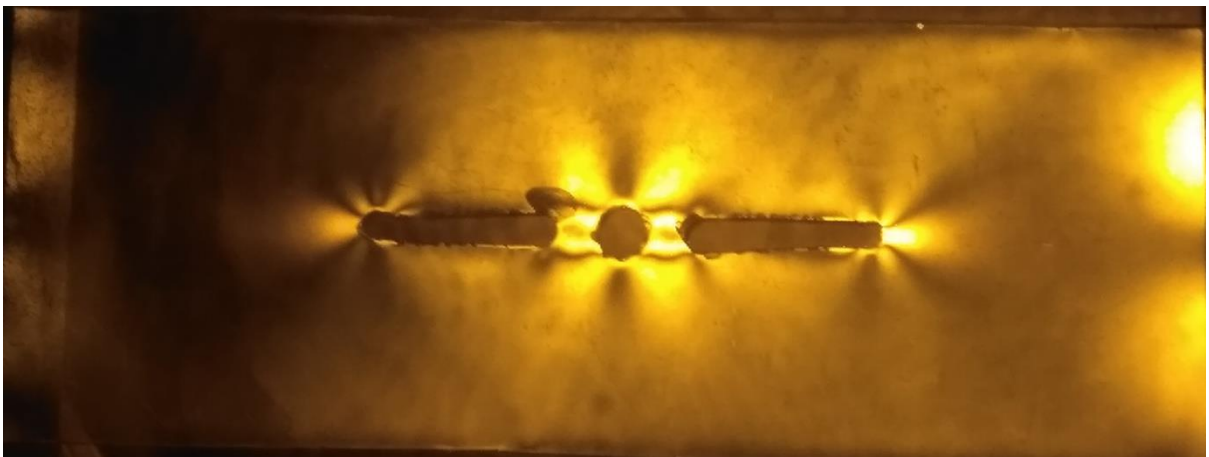


Fig.34 Third Order (monochromatic)

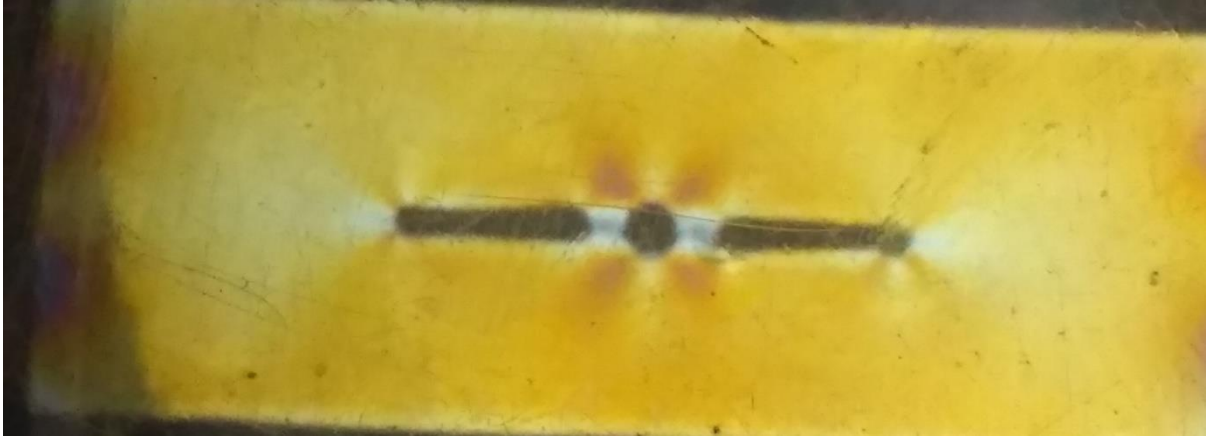


Fig.35 First Order (white light)

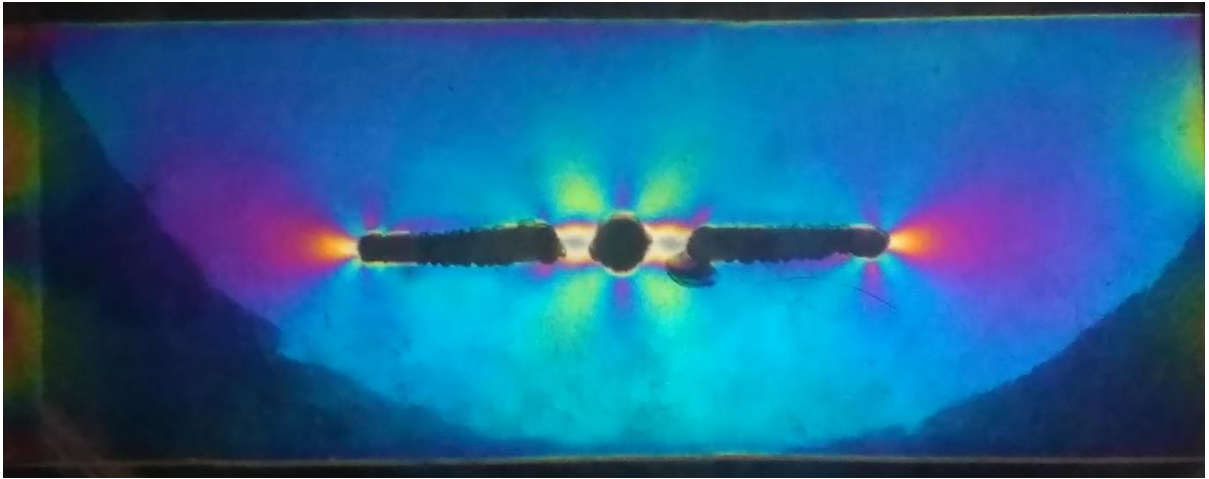


Fig.36 Second Order (white light)

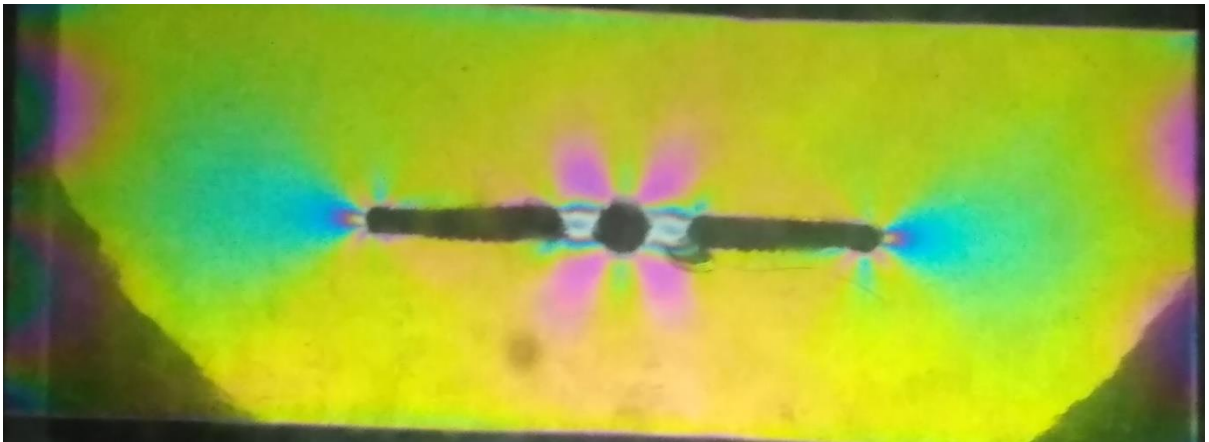


Fig.37 Third Order (white light)

5.3 Variation of SCF with Length of trapezoidal hole:

L=20 mm

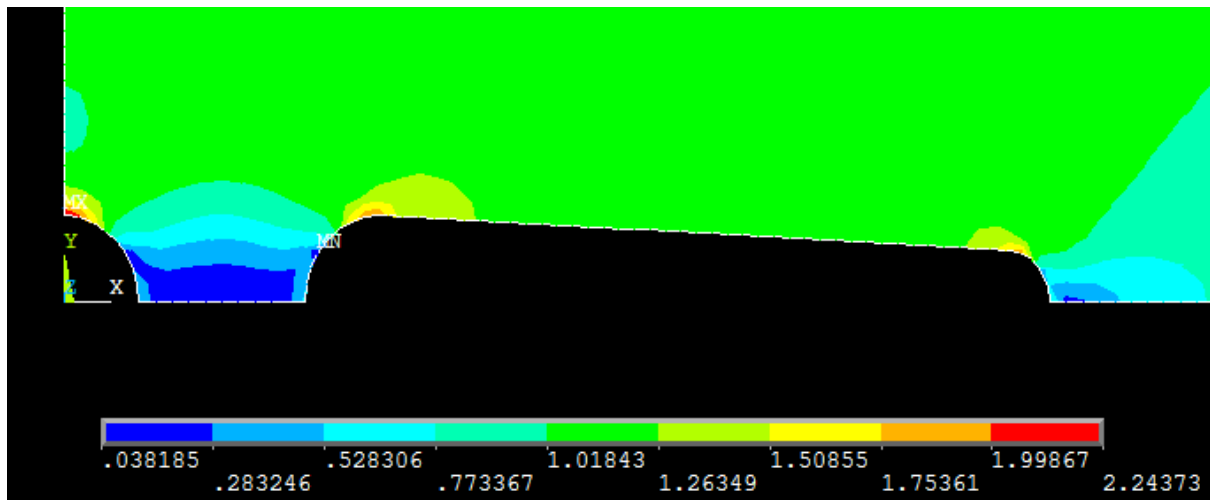


Fig.38 Stress distribution for L=20mm

L=25mm

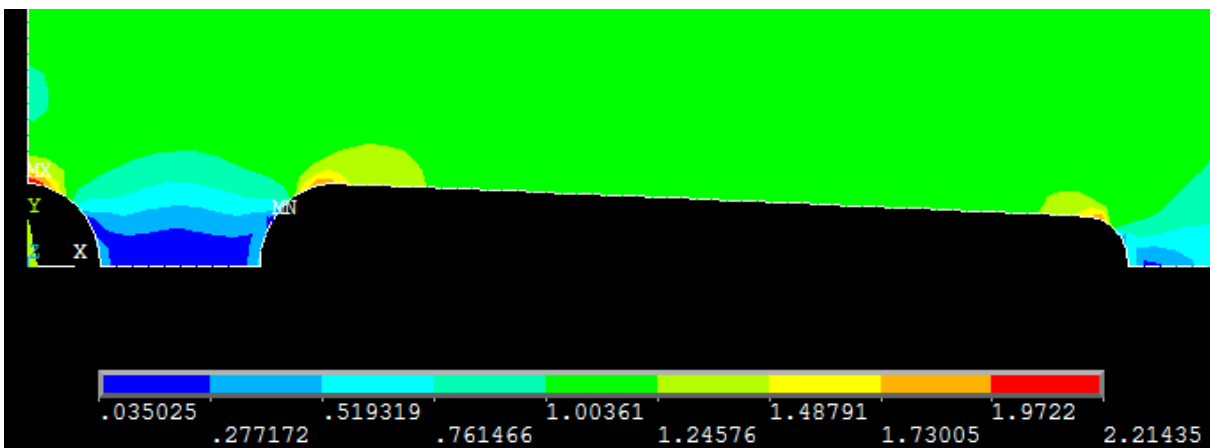


Fig.39 Stress distribution for L=25

L=30mm

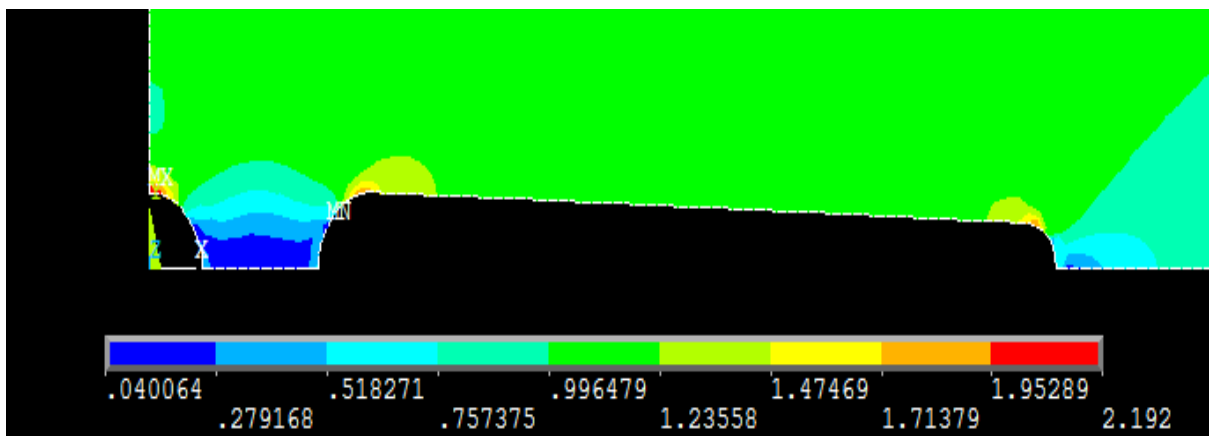


Fig.40 Stress distribution for L=30

L=35mm

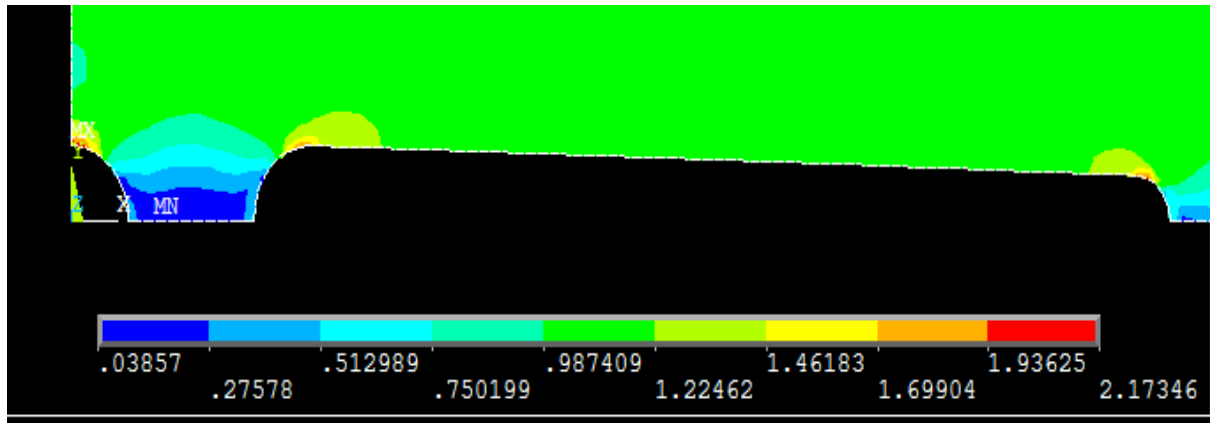


Fig.41 Stress distribution for L=35

L=40mm

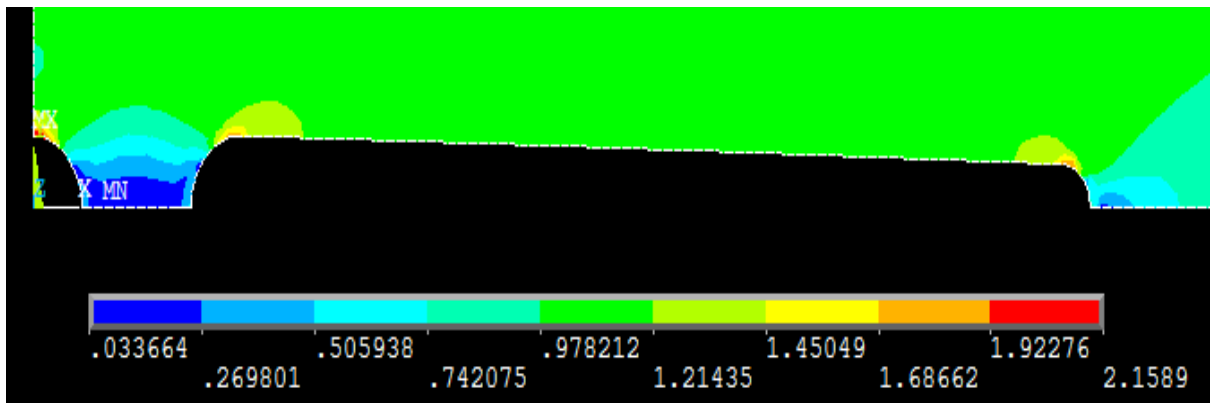


Fig.42 Stress distribution for L=40

L=45mm

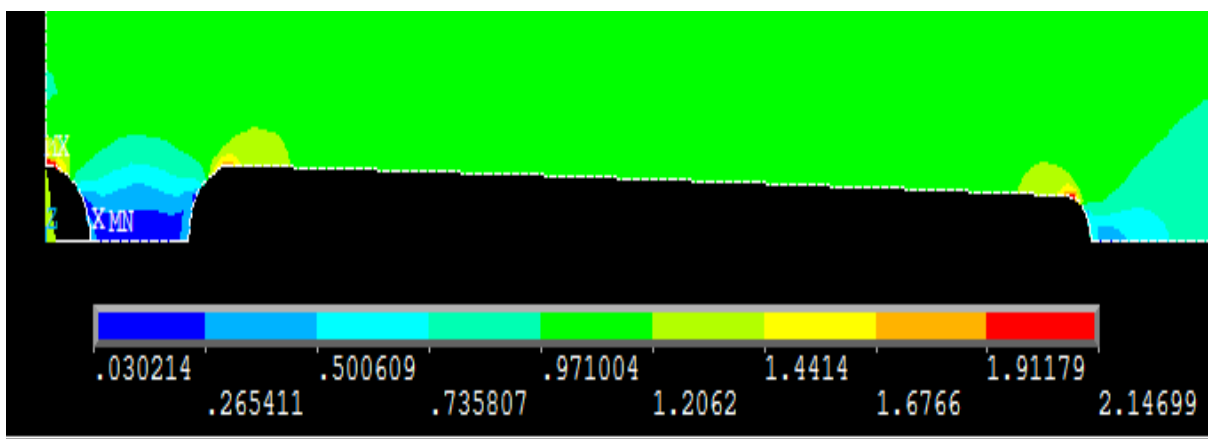


Fig.43 Stress distribution for L=45

L=50mm

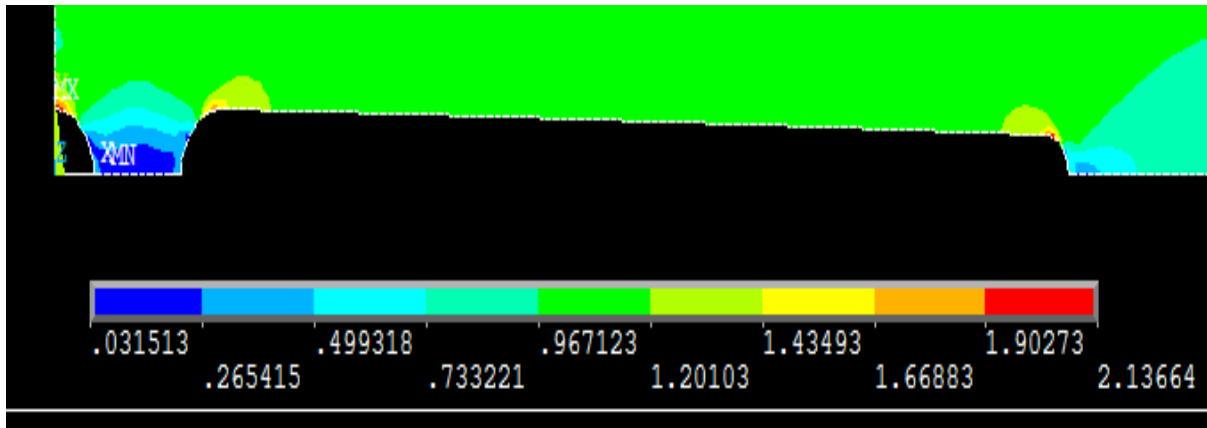


Fig.44 Stress distribution for L=50

L=55mm

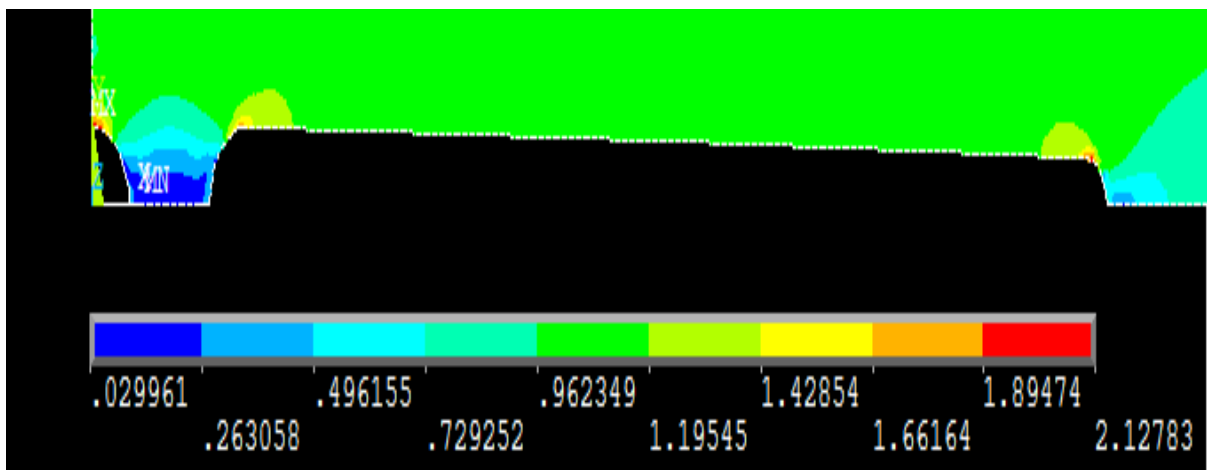


Fig.45 Stress distribution for L=55

L=60mm

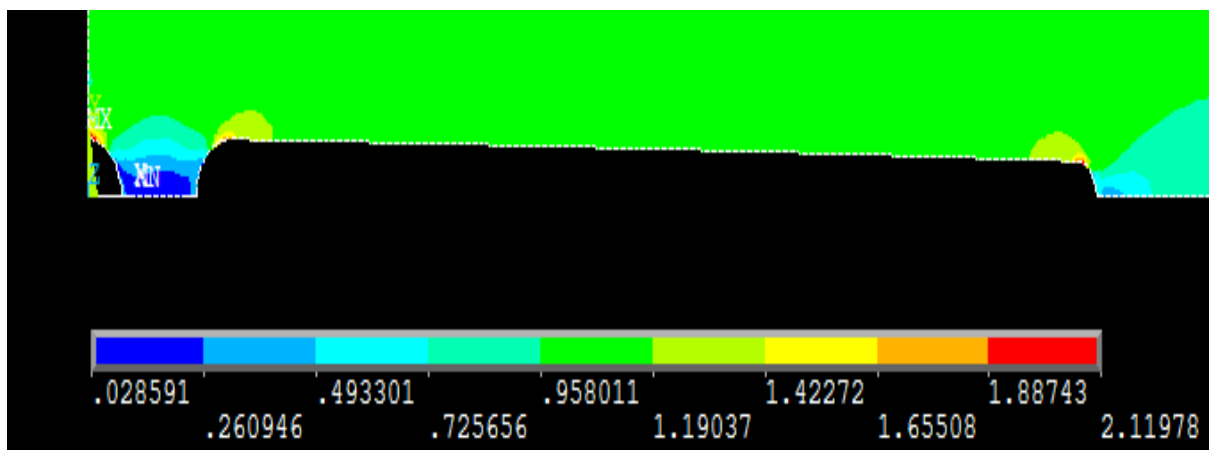


Fig.46 Stress distribution for L=60

L=65mm

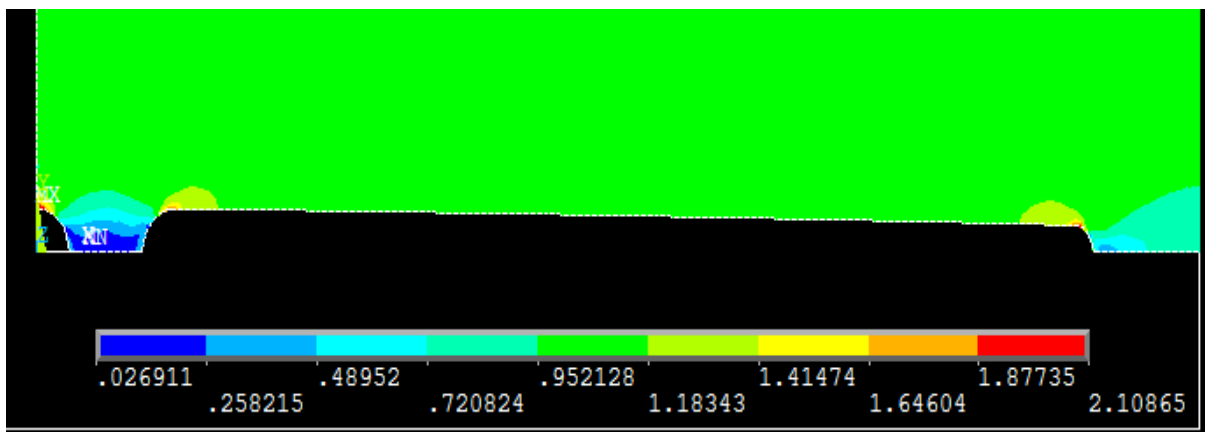


Fig.47 Stress distribution for L=65

L=70mm

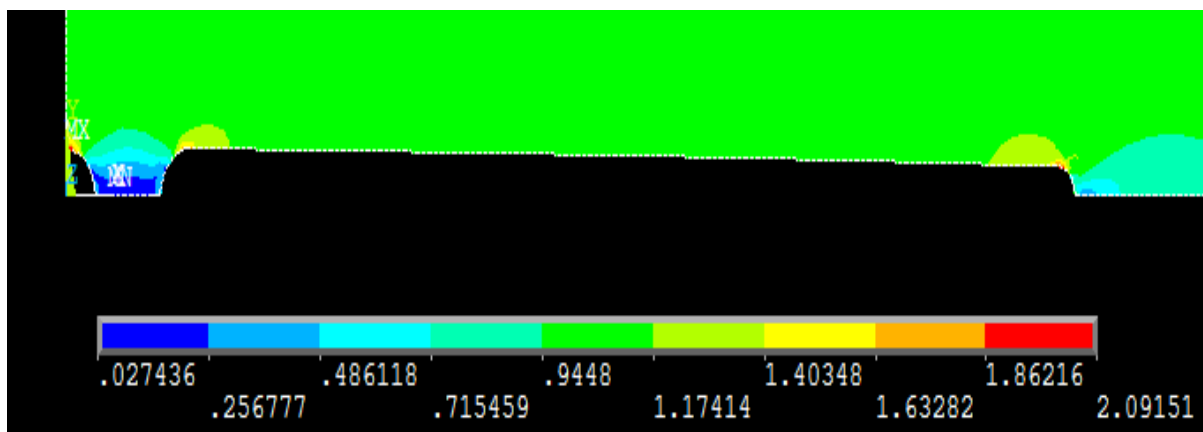


Fig.48 Stress distribution for L=70

L=75mm

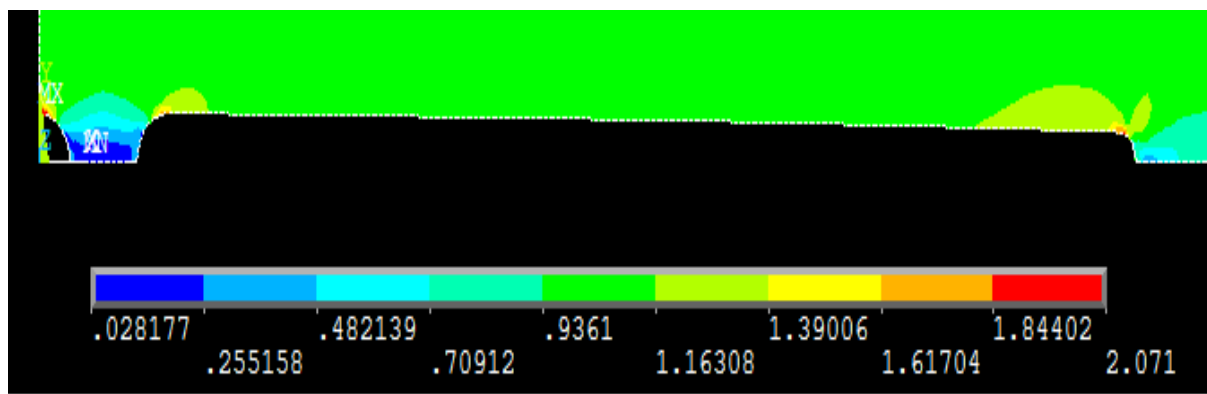


Fig.49 Stress distribution for L=75

Table.11 SCF for different L values

<i>Length (L)</i>	<i>Maximum stress</i>	<i>SCF</i>	<i>% reduction in SCF</i>
20	2.24	2.016	25.05
25	2.21	1.99	26.02
30	2.19	1.97	26.76
35	2.17	1.95	27.50
40	2.16	1.94	27.88
45	2.147	1.93	28.25
50	2.136	1.92	28.62
55	2.127	1.914	28.84
60	2.119	1.907	29.10
65	2.108	1.897	29.47
70	2.09	1.881	30.07
75	2.07	1.863	30.74

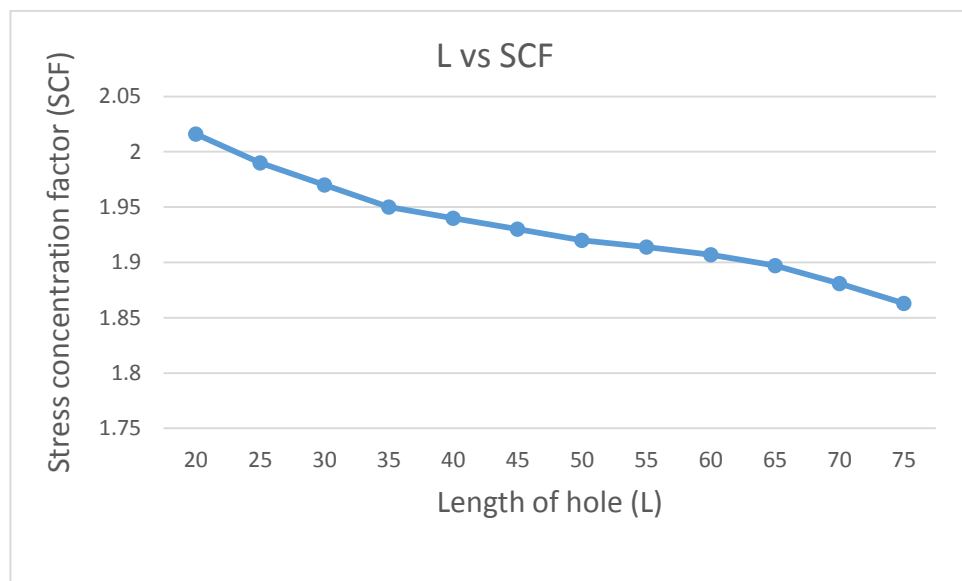


Fig.50 Plot L vs SCF

5.4 Variation of SCF with peripheral distance:

X=5mm

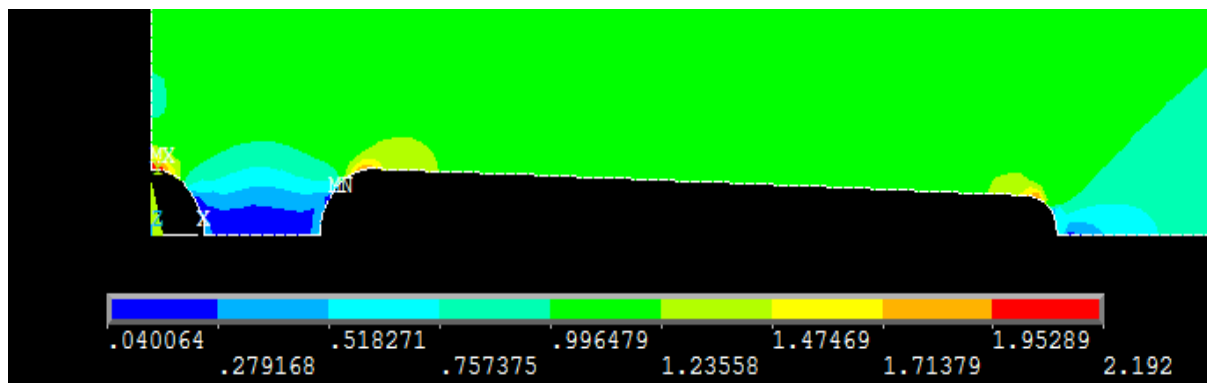


Fig.51 Stress distribution for X=5

X=4mm

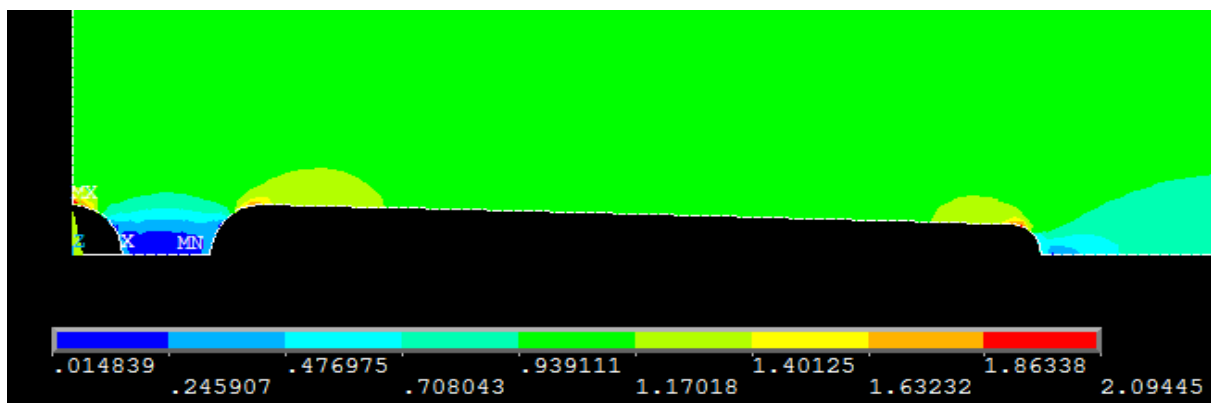


Fig.52 Stress distribution for X=4

X=3mm

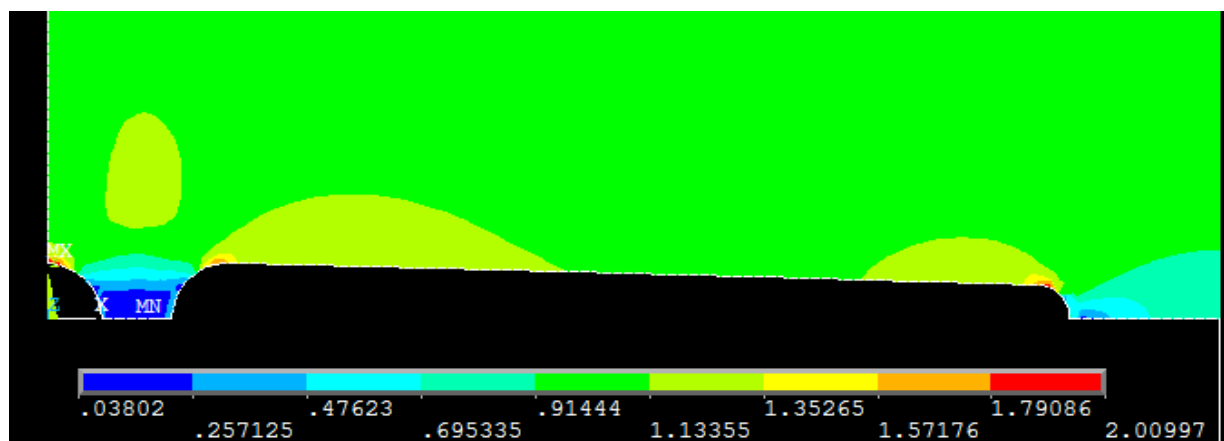


Fig.53 Stress distribution for X=3

X=2mm

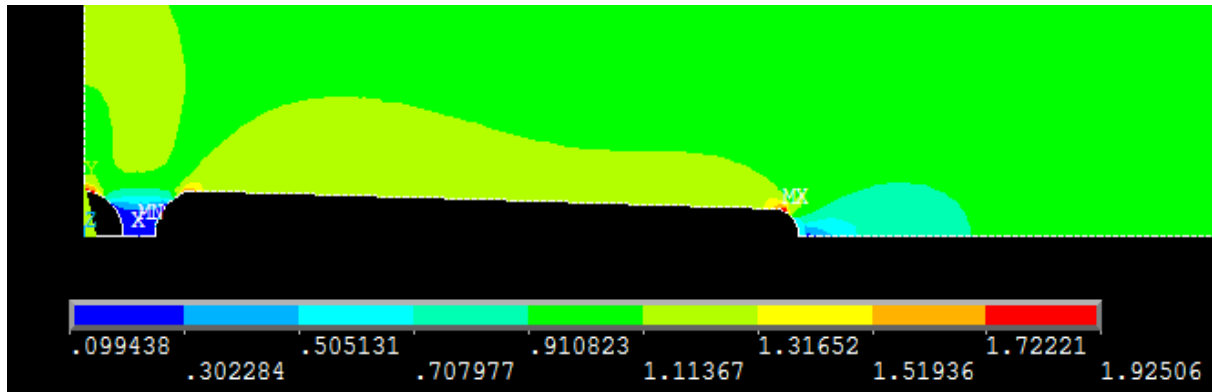


Fig.54 Stress distribution for X=2

X=1mm

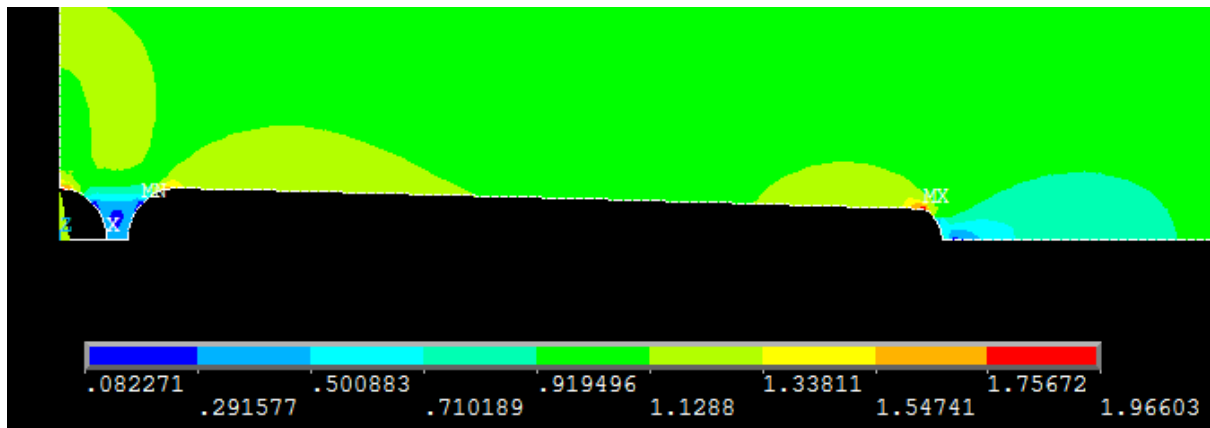


Fig.55 Stress distribution for X=1

X=0mm

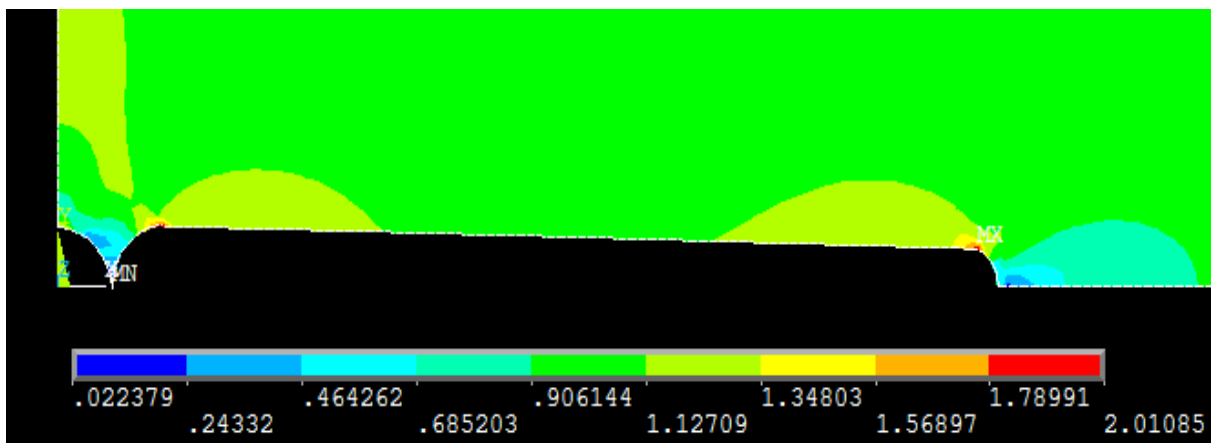


Fig.56 Stress distribution for X=0

Table.12 SCF for different X values

<i>Peripheral distance (X)</i>	<i>Maximum stress</i>	<i>SCF</i>	<i>% reduction in SCF</i>
5	2.19	1.97	26.76
4	1.884	1.884	29.96
3	1.808	1.808	32.78
2	1.732	1.732	35.61
1	1.769	1.769	34.23
0	2.01	1.801	33.04

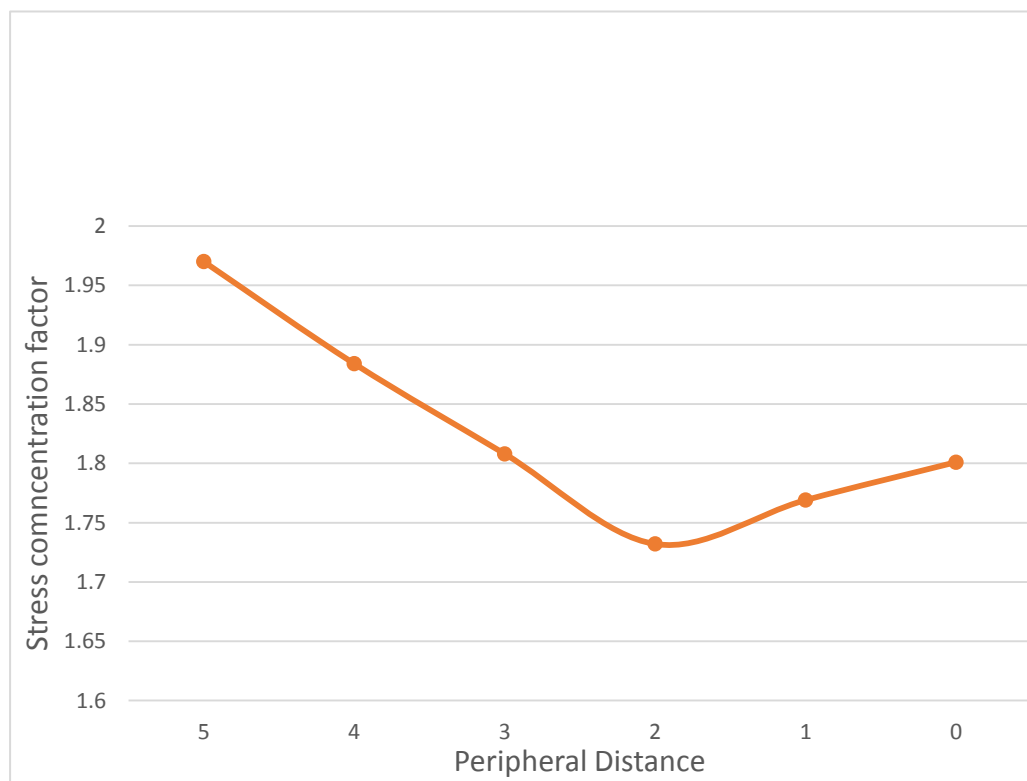


Fig.57 Plot X vs SCF

6. Conclusion

- Finite element analysis of rectangular plate was performed and results has been validated by photoelastic experimentation.
- The results obtained from finite element analysis was found close to that of photoelastic experimentation, so the finite element analysis is used for further work.
- From the analysis we found that by increasing the length of trapezoidal hole, stress concentration factor reduces.
- It is also found that on reducing the peripheral distance between main hole and trapezoidal auxiliary hole, the stress concentration factor reduces initially but as the two holes come too closer, increase in stress concentration factor was observed.
- In our analysis, reduction in stress concentration factor up to 35.6% was observed, which is significantly greater than other optimized designs.

7. References

1. K. Rajaiah and A. J. Durelli, "Optimum hole shapes in finite plates under uni-axial load," *Applied Mechanics*, vol. 46(3), pp. 691-695, 1979.
2. K. Rajaiah and N. K. Naik, "Hole Shape optimization in a finite plate in the presence of auxiliary holes," *Experimental Mechanics*, pp. 157-161, June 1984.
3. N. Troyani, C. Gomes, and G. Sterlacci, "Theoretical stress concentration factors for short rectangular plates with centered circular holes," *Journal of Mechanical Design*, vol. 124, March, 2002.
4. Shubhrata Nagpal, Nitin Jain and Shubhashis Sanyal- Stress concentration and its mitigation techniques in flat plate with singularities of Engineering Journal
5. S. A. Meguid, "Finite element analysis of defence hole systems for the reduction of stress Concentration in a uniaxially-loaded plate with coaxial holes," *Engineering Fracture Mechanics*, vol. 25, no. 4, pp. 403-413, 1986.
6. Kambale and Gulhane "Relief holes for the mitigation of stress concentration factor of a thin rectangular plate under in-plane loading."
7. N.K. Jain. "3D analysis of stress concentration factor and deflection in thin isotropic and orthotropic plates with central circular hole subjected to transverse loading". *IJMERD*, Vol. 1, No. 6, 2011, p. 01-13.
8. R. B. Heywood, *Designing by Photoelasticity*, pp. 296-298. Chapman & Hall (1952).
9. Moon Banerjee, N.K. Jain and S. Sanyal . "Three dimensional parametric analyses on effect of fibre orientation for stress Concentration factor in fibrous composite cantilever plate with central circular hole under transverse loading". *IIUM Engineering Journal*, Vol. 13, No. 2, 2012.

10. A. I. Zirka, M. P. Malezhik, and I. S. Chernyshenko, "Stress distribution in an orthotropic plate with circular holes under impulsive loading," *International Applied Mechanics*, vol. 40, no. 2, 2004.
11. Roark R. J., "Formulae for stress and strain", 4th edition, McGraw Hill.
12. A.M. Wahl, Beeuwkes Jr., East Pittsburgh, - Testing of stress concentration by photo elastic apparatus.
13. Peterson's Stress concentration factors – Third edition by Walter D, Pilkey and Deborah F. Pilkey
14. Erratum: Theoretical stress concentration factor for short rectangular plate with centred circular hole.
15. R E Peterson. 'Stress concentration design factors'. John Wiley and sons, New York.
16. G. S. Giare and R. Shabahang, "The reduction of stress concentration around the hole in an isotropic plate using composite material," *Engineering Fracture Mechanics*, vol. 32, no. 5, pp. 757-766, 1989.
17. S. Sanyal and P. Yadav, "Relief holes for stress mitigation in infinite thin plate with single circular hole loaded axially," *ASME International Mechanical Engineering Congress & Exposition*, 2005.